First Measurements of Organic Triplet Excited States in Atmospheric Waters

R. Kaur[†,‡] and C. Anastasio[†,‡,*]

[†]Department of Land, Air and Water Resources, University of California-Davis, One Shields Avenue, Davis, CA 95616-8627, USA

[‡]Agricultural and Environmental Chemistry Graduate Group, University of California-Davis, One Shields Avenue, Davis, CA 95616-8627, USA

Correspondence to: C. Anastasio (canastasio@ucdavis.edu)

ABSTRACT

Photooxidants chemically transform organic compounds in atmospheric drops and particles. Photooxidants such as hydroxyl radical ($^{\bullet}OH$) and singlet molecular oxygen ($^{1}O_2^*$) have been characterized in cloud and fog drops, but there are no measurements of the triplet excited states of organic matter ($^{3}C^*$). These "triplets", which are formed from excitation of chromophoric dissolved organic matter (CDOM), i.e., brown carbon, are difficult to measure because they are a mixture of species instead of a single entity. Here, we use a two-probe technique to measure the steady-state concentrations, rates of photoformation and quantum yields of oxidizing triplet states during simulated-sunlight illumination of bulk fog waters. Concentrations of $^{3}C^*$ are (0.70 ─ 15) × 10^{-14} M with an average (± σ) value of 5.0 (± 5.1) × 10^{-14} M. The average $^{3}C^*$ photoformation rate is 130 (± 130) μM h^{-1}, while the average quantum yield is 3.7 (± 4.5) %. Based on our previous measurements of $^{\bullet}OH$ and $^{1}O_2^*$ in the same fog samples, the ratio of the steady-state concentrations for $^{1}O_2^*$: $^{3}C^*$: $^{\bullet}OH$ is approximately 3 : 1 : 0.04, respectively. At our measured concentrations, triplet excited states can be the dominant aqueous oxidants for organic compounds such as phenols from biomass combustion.

INTRODUCTION

Fog drops, cloud drops, and aqueous particles are important sites for the photochemical cycling of carbon and nitrogen,[1-3] and the formation of aqueous secondary organic aerosol (SOA(aq)).[4-9] Many of these reactions are driven by photochemically-generated oxidant species (photooxidants), which include hydroxyl radical ($^{\bullet}OH$), singlet molecular oxygen ($^1O_2^*$), superoxide/hydroperoxyl radical ($^{\bullet}O_2^{-}/HO_2^{\bullet}$), hydrogen peroxide (HOOH), and triplet excited states of organic matter ($^3C^*$). Triplet excited states are formed when chromophoric dissolved organic matter (CDOM), i.e., brown carbon, absorbs (sun)light and is promoted from the singlet ground state to (eventually) a more reactive, excited triplet state. Subsequent triplet reactions occur mainly via two pathways – energy transfer and electron transfer. One example of the former is the transfer of energy from an organic triplet excited state to dissolved molecular O_2 to form singlet oxygen.[10] The second pathway, triplet-induced oxidation, is especially rapid with organics such as anilines or phenols, via one-electron or proton-coupled electron abstraction, respectively.[11-13] In this work we are studying oxidizing triplet states, which (for simplicity) we will generally refer to as "triplets" or "$^3C^*$"; in contrast, we will explicitly state "energy-transfer" triplet states when referring to this larger pool.

While there are some measurements of $^{\bullet}OH$, $^1O_2^*$, and HOOH in fog,[14, 15] cloud,[16-18] rain[19, 20] and aqueous extracts of particles,[21-24] there are no measurements of triplet excited states in atmospheric waters. One study attempted to measure triplets in illuminated rain waters,[20] but concentrations were too low to be observed. In contrast, there are numerous studies of triplets in surface waters, where they are significant oxidants for numerous classes of organics, including anilines, phenylurea herbicides and heterocyclic sulfur-containing compounds.[11, 25-29]

Although there are no measurements of triplet excited states in atmospheric particles or drops, laboratory studies have shown that triplets can oxidize isoprene and its oxidation products,[30,31] form hydrogen peroxide,[32] and produce low volatility species that constitute SOA(aq).[33, 34] However, laboratory studies typically use very high concentrations of triplet precursors, which are likely far above environmental levels. For example, while particles containing millimolar concentrations of imidazole-2-carboxaldehyde (a triplet precursor) can oxidize isoprene and its products to form appreciable amounts of SOA during laboratory illumination,[35, 36] a model of the same chemistry under atmospherically relevant conditions shows negligible SOA formation.[37] Understanding the roles and significance of triplet excited states in atmospheric chemistry requires that we know their steady-state concentrations. In addition, since “triplets” represent a heterogeneous class of reactive species with a wide range of reactivities,[38] it is also important to know the reactivities of triplets.

To address these needs, here we characterize triplet excited states of organic matter in bulk fog waters from two locations: Davis, California, and Baton Rouge, Louisiana. We recently reported on the kinetics and concentrations of hydroxyl radical and singlet oxygen in the same samples.[14] In this work our goals are to (i) develop a technique to measure the concentrations and reactivities of oxidizing triplets using two probe molecules, (ii) measure the steady-state concentrations, reactivities, rates of photoformation, and lifetimes of triplet excited states, and (iii) use our measurements to compare the importance of $^3C^*$, $^{\bullet}OH$, and $^1O_2^*$ as oxidants in atmospheric drops.

MATERIALS AND METHODS

Chemicals. Syringol (99%) and methyl jasmonate (≥ 95%) were purchased from Sigma-Aldrich and were used as received. Solutions were prepared using purified (Milli-Q) water from a Milli-Q Plus system (Millipore; ≥18.2 MΩ cm) with an upstream Barnstead activated carbon cartridge.

Fog Collection and Characterization. Sample collection and processing are discussed in detail in a previous paper.[14] Twelve samples (8 fogs and 4 field blanks) were collected in Davis, California (38.5539° N, 121.7381° W, 16 m above sea level) and Baton Rouge, Louisiana (30.4500° N, 91.1400° W, 17 m ASL) using stainless steel Caltech Active Strand Cloudwater Collectors, filtered using 0.45 μm

PTFE membranes (Pall Corporation), flash-frozen with liquid nitrogen, and stored in a –20 °C freezer until illumination. Major anions and cations were quantified using two Metrohm ion chromatographs (881 Compact IC Pro) equipped with conductivity detectors.[39, 40] Dissolved organic carbon (DOC) was measured using a Shimadzu TOC-VCPH analyzer.[39] Solution pH was measured using an Orion model 420A pH meter and light absorption was measured using a Shimadzu UV-2501PC spectrophotometer. Fog sample collection and composition data are shown in Table S1 of the Supporting Information and were discussed in a previous paper.[14]

Sample Illumination and Chemical Analysis. Air-saturated fog water samples were spiked with a triplet probe (see below), aliquoted into airtight 1-cm quartz cuvettes (Spectrocell) at 25 °C with constant stirring, and illuminated with a 1000 W Xenon arc lamp filtered with an AM 1.0 air mass filter (AM1D-3L, Sciencetech) and 295 nm long-pass filter (20CGA-295, Thorlabs) to mimic tropospheric solar light (Figure S1). Aliquots of illuminated (and parallel dark) samples were periodically removed and analyzed for the concentration of triplet probe using HPLC (Shimadzu LC-10AT pump, ThermoScientific BetaBasic-18 C_{18} column (250 × 33 mm, 5 µm bead), and Shimadzu-10AT UV-Vis detector). The daily photon flux was measured using a 10 µM solution of 2-nitrobenzaldehyde (2NB).[41]

Triplet Determination. In each sample we used two probes – syringol (SYR), a phenol, and methyl jasmonate (MeJA), an aliphatic alkene – to determine triplet concentrations and reactivities. SYR is an electron-rich phenol that reacts rapidly with triplets and is similar to 2,4,6-trimethylphenol (TMP), which has been used to measure triplet activity in surface waters.[11, 42] . As the second triplet probe we chose MeJA, an unsaturated aliphatic compound emitted by green plants that reacts with triplets.[43] Although MeJA does not react with triplets as rapidly as does SYR (and the mechanism for the MeJA reaction is unknown), it is useful as a probe because its rate constant with triplets is more sensitive to triplet reactivity than is the case for SYR. As we discuss below, we use this difference in SYR and MeJA reactivities with oxidizing triplets to better constrain triplet concentrations and determine their average reactivity in each sample. However, because MeJA reacts less quickly with triplets, it is subject to more degradation from other oxidants; although we correct for the $^{\bullet}$OH and $^1O_2$* contributions, the relatively large size of these corrections adds uncertainty to the MeJA-derived triplet concentrations.

In experiments, two separate 5 mL portions of each fog sample were spiked with 2 μM of one probe, illuminated, and aliquots were removed at known time intervals. The concentration of probe was kept low to avoid perturbing the steady-state concentrations of photooxidants. Parallel dark controls were performed with every experiment: an aluminum foil-wrapped cuvette containing the probe-spiked sample was placed inside the illumination chamber for the duration of the illumination and aliquots were analyzed at regular intervals. The concentration of SYR or MeJA was measured in each illuminated and dark aliquot using HPLC-UV (SYR: 20% acetonitrile / 80% water for eluent, detection wavelength 210 nm; MeJA: 50% acetonitrile / 50% water for eluent, detection wavelength 200 nm; flow rate of 0.6 mL min^{-1} for both probes). In all samples, the loss of probe followed first-order kinetics: the rate constant for loss of probe, $k'_{Probe,EXP}$ (s^{-1}), was determined as the negative of the slope of the regression line of $\ln([Probe]_t/[Probe]_0)$ versus t. Each $k'_{Probe,EXP}$ was normalized to the value expected under midday Davis, CA winter solstice sunlight using 2-nitrobenzaldehyde (2NB) actinometry:[41]

$$k'_{Probe} = k'_{Probe,EXP} \times \frac{j_{2NB,WIN}}{j_{2NB,EXP}} \qquad (1)$$

where $j_{2NB,WIN}$ is the rate constant for loss of 2NB measured at midday near the winter solstice in Davis ($0.0070\ s^{-1}$)[15] and $j_{2NB,EXP}$ is the measured rate constant for loss of 2NB on the day of the experiment. While first-order rate constants for probe loss, and the accompanying steady-state concentrations of ^3C*, $^{\bullet}$OH, and $^1O_2$* described below, are all Davis winter-solstice normalized, we omit the "WIN" subscript for simplicity. The hydroxyl radical and singlet oxygen measurements in the same fog samples are discussed in our companion paper and given in Table S2.[14] The Davis winter solstice-normalized SYR and MeJA loss kinetics are given in Tables S3, S4 and S5.

Since both triplet probes also react with other oxidants, the measured (and normalized) rate constant for loss of each probe is the sum of all of loss pathways, including reaction with $^{\bullet}OH$, $^{1}O_2^*$, direct photodegradation, and other oxidants:

$$k'_{Probe} = k_{Probe+OH}[^{\bullet}OH] + k_{Probe+1O2^*}[^{1}O_2^*] + \Sigma(k_{Probe+3C_i^*}[^{3}C_i^*]) + j_{Probe} + \Sigma(k_{Probe+Other}[Other]) \qquad (2)$$

In this equation - and throughout this work – we use the prime notation to denote a pseudo-first-order rate constant (e.g., k'_{Probe}) and the notation k_{A+B} (e.g., $k_{Probe+OH}$) to denote a second-order rate constant. To remove the reactivity contributions of $^{\bullet}OH$ and $^{1}O_2^*$ from k'_{Probe} (eq 2), we measured their concentrations in our companion paper[14] and used second-order rate constants $k_{Probe+OH}$ and $k_{Probe+1O2^*}$ for both probes from the literature (Table S6 of the SI). The term $\Sigma(k_{Probe+3Ci^*}[^{3}C_i^*])$ in eq 2 represents the sum of the oxidizing triplet contributions to probe loss, while j_{Probe}, the first-order rate constant for direct photodegradation of the probes, is negligible for our illumination times (with values below 3.6×10^{-6} and 2.5×10^{-7} s^{-1} for SYR and MeJA, respectively, under Davis winter conditions). The final term in eq 2 is the sum of contributions from other oxidants; as discussed later, these contributions appear to be minor, representing at most only 7% of SYR loss. Based on this, we determine the pseudo-first-order rate constant for loss of each probe due to reaction with triplets by simplifying and re-arranging eq 2:

$$k'_{Probe,3C^*} = \Sigma(k_{Probe+3C_i^*}[^{3}C_i^*]) = k'_{Probe} - (k_{Probe+OH}[^{\bullet}OH] + k_{Probe+1O2^*}[^{1}O_2^*]) \qquad (3)$$

This pseudo-first-order rate constant for probe loss due to triplets is composed of contributions from each triplet excited state in a given sample, i.e.,

$$k'_{\text{Probe},3\text{C}^*} = (k_{\text{Probe+3C}_1^*} \times [^3\text{C}_1^*]) + (k_{\text{Probe+3C}_2^*} \times [^3\text{C}_2^*]) + (k_{\text{Probe+3C}_3^*} \times [^3\text{C}_3^*]) + \ldots \quad (4)$$

Normally, in techniques where the loss of probe is measured (e.g., for $^1O_2^*$) the concentration of oxidant is determined by dividing the measured pseudo-first-order rate constant for probe loss by the second-order rate constant for reaction of probe with oxidant. The equivalent equation for the concentration of triplet excited states from each probe is:

$$\Sigma[^3\text{C}_i^*]_{\text{Probe}} \approx \frac{k'_{\text{Probe},^3\text{C}^*}}{k_{\text{Probe}+^3\text{C}^*}} \quad (5)$$

However, determining triplet steady-state concentrations is not as straightforward, since multiple triplet excited states contribute to the loss of probe, each with its own second-order rate constant for reaction with the probe compound; i.e., there are multiple values of $k_{\text{Probe+3C}^*}$ in eq 5. Since we do not know the identities or rate constants of the natural triplets, in the denominator of eq 5 we use second-order rate constants for the triplet states of four model compounds:[27, 39, 44] 2-acetonaphthone (2AN), 3'-methoxyacetophenone (3MAP), 3,4-dimethoxybenzaldehdye (DMB), and benzophenone (BP). The second-order rate constants of their triplet excited states with syringol and methyl jasmonate ($k_{\text{Probe+3C}^*}$) span ranges of (1.9 to 8.5) × 10^9 and (0.019 to 5.1) × 10^9 $M^{-1}s^{-1}$, respectively (Table S6).[42-44] We measured second-order rate constants for cases not previously reported, using a relative rate technique[43, 45] that is described in section S1; the rate constants for all model triplet species were determined independently from each other, in separate experiments. By using two probes we can estimate the average reactivity for triplets in a given sample: more reactive triplets react similarly fast with both probes, while less reactive triplets show larger differences in their SYR and MeJA rate constants. For example, in case of the model triplets, values of the second-order rate constant ratio $k_{\text{SYR+3C}^*}$ / $k_{\text{MeJA+3C}^*}$ for ^{3}2AN*, ^{3}3MAP*, ^{3}DMB* and ^{3}BP* are 100, 32, 8.5, and 1.7, respectively (Table S5): the most reactive model triplet (^{3}BP*) has a ratio closer to unity, while our least reactive triplet (^{3}2AN*) has a large ratio. By the same logic, in natural samples the pseudo-first-order rate constant ratio (i.e., $k'_{SYR,3C*}$ / $k'_{MeJA,3C*}$) is an indicator of the average reactivity of the triplet mixture in that sample.

We determine the concentration of oxidizing triplets using their average reactivity in each sample through four steps: (1) Use the ratio $k'_{SYR,3C*}$ / $k'_{MeJA,3C*}$ to determine the "best triplet matches", i.e., the two model triplets ($^3C_1$* and $^3C_2$*) that most closely resemble the average reactivity of the triplet mixture in a sample. This is done by finding the two model triplets whose ratio of second-order rate constants for reaction with the probes (i.e., $k_{SYR+3C*}$ / $k_{MeJA+3C*}$) brackets the ratio of triplet probe first-order rate constants for loss (i.e., $k'_{SYR,3C*}$ / $k'_{MeJA,3C*}$). (2) In the second step, using the rate constants of the best triplet matches, we calculate the mole fractions (χ_{3C1*} and χ_{3C2*}) of the two best match triplets so that

$$\frac{k'_{SYR,3C^*}}{k'_{MeJA,3C^*}} = \frac{\chi_{3C1^*} \times k_{SYR+3C1^*} + \chi_{3C2^*} \times k_{SYR+3C2^*}}{\chi_{3C1^*} \times k_{MeJA+3C1^*} + \chi_{3C2^*} \times k_{MeJA+3C2^*}} \quad (6)$$

where $k_{Probe+3C1*}$ and $k_{Probe+3C2*}$ are the second-order rate constants of the best model triplet matches with each probe. Since in our simplified scheme $\chi_{3C2*} = 1 - \chi_{3C1*}$, we can rearrange eq 6 to solve for the mole fractions:

$$\chi_{3C1^*} = \frac{k_{SYR+3C2^*} - \left(\frac{k'_{SYR,3C^*}}{k'_{MeJA,3C^*}}\right) k_{MeJA+3C2^*}}{\left(\frac{k'_{SYR,3C^*}}{k'_{MeJA,3C^*}}\right)(k_{MeJA+3C1^*} - k_{MeJA+3C2^*}) + k_{SYR+3C2^*} - k_{SYR+3C1^*}} \quad (7)$$

(3) In the third step, we use the mole-fraction-weighted second-order rate constants for each probe (i.e., from eq 6, the numerator for SYR or denominator for MeJA) to calculate the triplet concentration in each sample based on each probe:

$$\Sigma[^3C_i^*]_{Probe} = \frac{k'_{Probe,3C^*}}{\chi_{3C1^*} \times k_{Probe+3C1^*} + \chi_{3C2^*} \times k_{Probe+3C2^*}} \quad (8)$$

(4) In the fourth and final step, we average the triplet concentrations derived from the two probes to obtain the best estimate of the oxidizing triplets steady-state concentration:

$$\Sigma[^3C_i^*] = \frac{\Sigma[^3C_i^*]_{SYR} + \Sigma[^3C_i^*]_{MeJA}}{2} \quad (9)$$

This technique and its underlying principles are described in greater detail in sections S2 and S3 of the supplemental information. Based on 15 hypothetical mixtures of the four model triplets, the best estimate of concentration from this technique is generally within 25% of the true concentration and always within a factor of two (Section S2 of the SI). In addition to giving a good estimate of the overall triplet concentration, the dual-probe technique also indicates the average apparent reactivity of the triplets in the fog samples. Using SYR alone as a probe gives similar – though less accurate – triplet concentrations compared to the two-probe technique (section 2.1 of the SI) but provides no information about the average reactivity of the triplets.

Finally, because we measure the triplet-mediated losses of SYR and MeJA, we are measuring only the oxidizing subset of triplet excited states. Since the triplet energy of SYR (likely 330 – 340 kJ mol^{-1} based on data for other electron-rich phenols[11]) is higher than typical CDOM triplet excited states (150 – 310 kJ mol^{-1})[11, 38] and our model triplets (249 – 303 kJ mol^{-1}; Table S7), we do not expect energy transfer to contribute to SYR loss. Similarly, while the triplet energy of MeJA is not known, given its slower reaction rate constants with the model triplets, its triplet energy is at least equal to that of SYR and thus energy transfer should also be negligible in MeJA loss.

Rate and Quantum Yield of Triplet Photoformation. Since the dominant natural sink of triplets is dissolved molecular oxygen,[11, 46, 47] we use the triplet concentration to calculate the winter-solstice-normalized rate of formation of oxidizing triplets, P_{3C*}, as:

$$P_{3C*} = \Sigma[^3C_i^*] \times (k_{3C*+O2} \times [O_2]) \quad (10)$$

where k_{3C*+O2} is an estimate, determined as the average rate constant for O_2 quenching for three model triplets (2.8 (± 0.4) × 10^9 $M^{-1}s^{-1}$; Table S7)[42, 44] and $[O_2]$ is the dissolved oxygen concentration (258 μM at 25 (± 1) °C).[42] We calculate the quantum yield of triplet formation (i.e., the fraction of photons absorbed by brown carbon that make an oxidizing triplet excited state) using

$$\Phi_{3C^*} = \frac{P_{3C^*}}{R_{abs}} \quad (11)$$

where R_{abs} is the rate of light absorption by the fog sample due to all chromophores (Table S2).[14] Our rate constant for triplet quenching by O_2 (k_{3C^*+O2}) is 40 % higher than the value estimated in surface waters by Zepp et. al.[48] Thus using the Zepp value would decrease our calculated triplet production rates and quantum yields by 30 % each.

Uncertainties. In figures, error bars represent ± 1 standard error (SE), calculated by propagating the uncertainties in each term used to determine the plotted value (i.e., as shown in the relevant equation).

RESULTS AND DISCUSSION

Probe Loss. Figure 1 illustrates results from a typical pair of triplet probe experiments in our fog waters: syringol decays more quickly than methyl jasmonate and there is no loss of either probe in the dark. Averaged across all of our samples except for LSU3, SYR loss is approximately 16 times faster than MeJA with average (± σ) rate constants of 1.5 (± 1.0) × 10^{-4} s^{-1} and 9.8 (± 2.0) × 10^{-6} s^{-1}, respectively (Table S3). Sample LSU3, the most acidic sample, is a notable outlier where SYR loss is less than 10% of the average value. There is a slow loss of SYR in one UCD field blank (representing 9% of the UCD sample mean rate constant), but no loss in the other three field blanks (Table S3).

$^{\bullet}OH$, $^1O_2$* and ^3C* Contributions to Probe Loss. To use measured losses of syringol and methyl jasmonate to determine concentrations of oxidizing triplet excited states, we need to first correct their measured loss rate constants for the contributions due to $^{\bullet}OH$ and $^1O_2^*$ (eq 3). As shown in Figure 2 (and Table S4), $^{\bullet}OH$ and $^1O_2^*$ together account for an average (± 1σ) of 16 (± 6) % of the winter-normalized loss rate constant for SYR (k'_{SYR}) across the fog samples (excluding LSU3), while triplets generally dominate SYR loss, accounting for an average of 84 (± 6) %. The previously mentioned sample LSU3 is an outlier here as well, with 95% of SYR loss due to $^{\bullet}OH$ and $^1O_2^*$. In the case of the slower reacting MeJA, $^{\bullet}OH$ and $^1O_2^*$ are more significant and together account for an average of 46 (± 16) % of the measured loss, while triplets account for an average of 54 (± 16) % (Figure 2 and Table S5). While we did not measure concentrations of other oxidants (e.g., hydroperoxyl radical and superoxide radical anion), based on our estimates, they together account for, at most, 7 % of the average measured syringol loss (section S4). Thus, it does not appear that oxidants other than $^{\bullet}OH$ and $^1O_2^*$ need to be considered in determining the contributions of triplet excited states to the losses of the triplet probes in these samples.

Excluding sample LSU3 (which has very large uncertainties), the average (± 1σ) pseudo-first-order rate constants for loss of SYR and MeJA due to oxidizing triplets ($k'_{Probe,3C^*}$) are 1.3 (± 0.9) × 10^{-4} and 5.3 (± 1.9) × 10^{-6} s^{-1}, respectively (Figure 3). Ratios of $k'_{SYR,3C^*}$ / $k'_{MeJA,3C^*}$ in these samples range from 4.9 to 110 and have an average (± 1σ) ratio of 34 (± 38) (Figure 3). As we discuss below, this ratio is a measure of the average reactivity of the mixture of triplets in a sample, with a ratio closer to unity corresponding to a more reactive triplet mixture.

Triplet Reactivities and Steady-State Concentrations. To estimate the overall steady-state concentration of oxidizing triplets ($\Sigma[^3C_i^*]$) using our $k'_{Probe,3C^*}$ measurements, we need a bimolecular rate constant for the reaction of triplets with each probe (eq 5). As described in the Methods and section S2, because we do not know *a priori* which rate constant is most representative of the fog water triplets, we use the rate constants for four model triplets – ^{3}2AN*,^{3}DMB*, ^{3}3MAP* and ^{3}BP* – to represent a wide range of natural triplet reactivities.

As shown in Figure 4, rate constants for these four triplets with syringol are all very fast, (1.9 – 8.5) × 10^9 M^{-1} s^{-1}, consistent with the relatively low reduction potential for easily oxidized phenols with electron-donating substituents.[11] In contrast, rate constants with methyl jasmonate are smaller and span a wider range since this probe is less easily oxidized, especially by the less reactive triplet states. As shown in the bottom panel of Figure 4, the four model triplet states span a wide range of ratios of bimolecular rate constants for reaction with SYR and MeJA, with the ratio $k_{SYR+3C*}$ / $k_{MeJA+3C*}$ decreasing with increasing triplet reactivity (i.e., triplet state reduction potential, Table S7). For ^{3}2AN*, the least reactive model triplet, this ratio is 100, while for ^{3}BP*, the most reactive model triplet, the ratio is only 1.7 (Figure 4, Table S6). Since this range of model triplet reactivities mimics the range measured for the fog triplets, where $k'_{SYR,3C*}$ / $k'_{MeJA,3C*}$ runs from 4.9 (± 2.9) to 110 (± 42) (Figure 3), it appears that our set of model triplets reasonably accounts for the range of average reactivities found in fog samples.

Using the four model triplet bimolecular rate constants for each of the two probes gives us two ranges of possible triplet steady-state concentrations for each sample, as shown by the blue and red lines in Figure 5. As described in SI sections S2 and S3, the two model triplets that most closely match the measured triplet probe reactivity in the fog samples (i.e., $k'_{SYR,3C*}$ / $k'_{MeJA,3C*}$) are the best matches for the average reactivity of the mixture of triplets in a given fog. We then use the mole-fraction weighted rate constants for these two model triplets to calculate the concentration of triplets from each probe (eqs 7–9). Excluding the outlier LSU3, the triplet concentrations calculated from SYR and MeJA are very close in a given sample - within 0.1% of each other except for UCD1, which has an RSD of 6% (Figure 5 and Table S11). The best estimate of the overall concentration of oxidizing triplets, $\Sigma[^{3}C_{i}*]$, in a given sample is then calculated as the average of the $\Sigma[^{3}C_{i}*]_{SYR}$ and $\Sigma[^{3}C_{i}*]_{MeJA}$ values from the best triplet match.

These best estimates of the oxidizing triplet concentrations are represented by the open circles in Figure 5 and are in the range of (0.70 – 15) × 10^{-14} M, with an overall average (± σ) of 5.0 (± 5.1) × 10^{-14} M (Table 1). The best match triplets provide insight into the reactivities of the fog triplets - the most common matches are ^{3}3MAP* and ^{3}DMB*, indicating that the average reactivity of the triplets in 6 of the 7 samples resembles the reactivity of these two model species. In general, the overall concentration of oxidizing triplets is inversely related to the reactivity of the best match triplets: samples with lower average reactivity triplets tend to have higher concentrations and vice versa (Figure S2). It is unclear whether this is an artifact of our technique or if this is a general trend for triplet excited states in atmospheric drops and particles. There are no previous reports of triplet concentrations in atmospheric drops or particles, but they have been estimated in illuminated surface waters, typically by employing probes that undergo energy transfer, e.g., by measuring the isomerization of 1,3-pentadiene[48] and sorbic acid (trans,trans-hexadienoic acid).[49] Triplet steady-state concentrations determined via such probes are reported to be in the range of $10^{-15} – 10^{-13}$ M. Grebel et. al. had samples which contained similar amounts of DOM as our fog waters (7.0 – 22 mg-C L^{-1}) reported concentrations of energy-transfer triplets in the range of (0.5 – 1.0) × 10^{-14} M, which is similar to our results although it is for a different population of triplets.[49] Based on the triplet energy (E_T) for sorbic acid and other diene probes (~ 250 kJ mol^{-1}), these probes likely measure only the high energy triplets, which are on average of 35% of the total triplet population in surface waters.[38] More generally, McNeill and Canonica[38] have suggested that in surface waters, the $[^1O_2^*]$ and total $\Sigma[^3C_i^*]$ concentrations are comparable since essentially all triplets can transfer energy to O_2 to form $^1O_2^*$. Based on our measured singlet oxygen concentrations in the fog samples (Table S4), the corresponding estimated range for the total triplet concentrations is 10^{-14} to 10^{-12} M. However this estimate includes triplets that can form $^1O_2^*$ (as all triplets likely can) but cannot oxidize organics. In contrast, we are reporting concentrations of only the subset of triplets that can oxidize syringol and methyl jasmonate.

To estimate the reactivity/selectivity of CDOM in natural waters, Canonica et. al. compared the relative rates for loss of electron-rich phenols in the presence of ^{3}2AN*, ^{3}3MAP* and ^{3}BP* as well as surface water DOM isolates.[11] They found that the average apparent selectivity (and thus reduction potential) of surface water DOM is very similar to ^{3}3MAP*. Our mole-fraction-weighted combinations for the fog samples suggest similar reactivity of triplets, with most samples having an average reactivity that is similar to that of ^{3}3MAP* and ^{3}DMB*.

As we describe in SI section S2, there are two important caveats of our technique: 1) The model best triplet matches (Table 1) give an indication of the average reactivity of the mixture of triplets in the sample and do not imply that all of the triplets in that sample are of that type. 2) As discussed in results for the hypothetical scenarios (section S2), the estimated triplet steady-state concentrations using our two-probe method are generally within 20% of the true value and always within a factor of two. The accuracy of the concentration is lowest if the mixture of triplets contains large fractions (>70%) of slow-reacting triplets, but, overall, triplet concentrations are rarely overestimated by our method. Since the $k'_{Probe,3C*}$ ratios are skewed by the higher rate constants of the highly reactive triplets, mixtures containing a majority of low-reactivity triplets can sometimes have an average triplet reactivity that resembles high-reactivity triplets. As a result, in this case the method gives lower triplet steady-state concentrations than the actual value. In contrast, based on our hypothetical scenarios, triplet concentrations are rarely over-estimated.

Triplet Photoproduction Rates and Quantum Yields. Based on the average rate constant for O_2 quenching of our model triplets (Table S7), we estimate that the first-order rate constant for quenching of fog triplets by molecular oxygen is 7.2 (± 1.1) × 10^5 s^{-1}. This is equivalent to an average triplet lifetime of 1.4 (± 0.2) μs, which is very similar to the average measured lifetime of $^{\bullet}OH$ in these samples (Table S2). Based on this, calculated rates of triplet photoproduction (P_{3C*}) range between 18 and 380 μM h^{-1} with an average value (± σ) of 130 (± 130) μM h^{-1} (eq 10); these values are very similar to the measured rates of $^1O_2*$ photoproduction (Table S2). In contrast, rates of $^{\bullet}OH$ formation in these samples are approximately 100 times slower (Table S2). A previous study attempted to measure $^3C*$ photoproduction rates in illuminated rain waters but found them to be at least 3 orders of magnitude lower (< 0.022 μM h^{-1}) than what we have measured here; rates of $^1O_2*$ photoformation were also very small (2.4 μM h^{-1}).[20] This difference is likely because the fog drops are much more concentrated in brown carbon compared to the more dilute rain drops. While triplets are formed from the photoexcitation of dissolved organic compounds, there is no correlation between DOC concentrations and the rate of triplet photoproduction (P_{3C*}) (Figure S3). This is likely due to the fact that $^3C*$ (and $^1O_2*$) yields vary significantly between different components of CDOM, which dominates light absorption (Figure S4). For the same reason, triplet quantum yields also vary widely, between 0.35% and 13%; on average, nearly 4% of the photons absorbed by the samples lead to triplet formation (Table 1). Surface water studies have reported similar triplet quantum yields, 1 – 10%, using both electron and energy-transfer probes,[49-51] indicating similarities in the chromophoric moieties of DOM in surface and atmospheric waters.

Energy Transfer and Electron Transfer Triplets. While our previous discussion focused on oxidizing triplets, as mentioned in the introduction, triplets can also undergo energy transfer. Here we use the quantum yields of $^1O_2$* and ^3C* to estimate the relative sizes of these two pools of triplet types. As discussed earlier, singlet oxygen is formed when triplet excited states of CDOM (i.e., brown carbon) transfer energy to molecular O_2.[10] Since the triplet states of most organic chromophores possess enough energy to accomplish this, all of the fog triplets can likely form $^1O_2$*,[38] although the yields of singlet oxygen vary (discussed below).[52] In contrast, we measure the triplets that can oxidize our probe molecules, which requires that the one-electron reduction potential of the triplet equals or exceeds the corresponding potential of the probe.[53] Thus, we expect that our probes measure only the electron-transfer subset of the total triplet pool. The ratio of the organic triplet excited state and singlet oxygen quantum yields should therefore approximately indicate the fraction of the entire triplet population that can oxidize our probes. More specifically, since only a fraction (f_Δ) of the interactions of a triplet excited state with dissolved O_2 results in formation of $^1O_2$*, [52] the quantum yield for formation of all triplets in our samples is $\Phi_{3C*(Total)} = \Phi_{1O2*}/f_\Delta$. While we do not know values of f_Δ for natural triplets in atmospheric samples, f_Δ for our model triplets ranges from 0.33 to 0.81 with an average (± 1σ) value of 0.53 (± 0.23) (Table S7), which is very similar to that seen in surface waters.[38] This suggests that the total triplet quantum yield is on the order of (2.1 – 23) % in our fog waters (Table 1, footnote *f*). In all seven samples, the fraction of total triplets that can oxidize organics (i.e., Φ_{3C*} / (Φ_{1O2*}/f_Δ)) ranges between 0.15 and 0.90 (Table 1), suggesting that electron-transfer triplets represent 15 – 90% of the total triplet pool. This is important because, unlike the electron transfer pathway, energy transfer from triplets to organic species is unlikely to oxidize the organic molecules and thus is unlikely to be a direct sink for organics. However, energy transfer from triplets to O_2 is the major source of $^1O_2*$,[54, 55] which can oxidize organic molecules.[14, 15, 55-57]

Implications. Our recent study on $^{\bullet}OH$ and $^1O_2*$,[14] combined with the current results for oxidizing triplet excited states, together represent the most comprehensive examination of photooxidants in atmospheric drops or particles. We can use the quantum yields for these different oxidants to characterize the fates of photons absorbed by the samples: on average, 4.2 % of the absorbed photons form $^1O_2*$, approximately the same percentage make triplets that are quenched by O_2 without making singlet oxygen (since $f_\Delta \sim 0.5$), 3.7 % form oxidizing triplets, and 0.035 % form hydroxyl radical. Thus, overall approximately 8 % of the total absorbed photons go lead to the formation of these three photooxidants, while the remainder goes towards other processes, including generation of heat.

Based on our measurements, the steady-state concentrations for the three photooxidants are in the order $^1O_2* > {^3C^*} > {^{\bullet}OH}$. Average singlet oxygen steady-state concentrations are three times higher than the triplets, and at these concentrations $^1O_2*$ can be a significant oxidant for atmospherically relevant organics such as polycyclic aromatic hydrocarbons and heterocyclic aromatic compounds, e.g., furans. On the other hand, average triplet steady-state concentrations are nearly 100 times higher than the hydroxyl radical formed in bulk fog (Table S4). Taking gas-to-aqueous transport of $^{\bullet}OH$ into account, the typical fog water $^{\bullet}OH$ concentration is estimated to be 2×10^{-15} M;[14] triplet concentrations would still be 25 times greater, making the latter the dominant oxidant for biomass-burning phenols such as syringol and guaiacol, which react at nearly diffusion-controlled rates with both $^{\bullet}OH$ and the high reactivity fog triplets. This is seen, for example, in Figure 2, where triplets are the dominant oxidant for SYR. Our results also show that concentrations of triplet excited states are high enough that these oxidants in fog are a significant sink for at least some unsaturated biogenic VOCs, such as methyl jasmonate. Understanding the broader importance of triplets as oxidants for atmospheric aqueous organics requires more measurements of bimolecular rate constants, of which there are currently few.[27, 42, 43, 58]

Finally, we suspect that triplet concentrations are even higher in aerosol liquid water compared to fog water. Recent work showed that triplet concentrations in laboratory ice samples are enhanced by a factor of nearly 100 relative to the same sample studied as solution, as a consequence of the concentration enhancement of triplet precursors in the liquid-like regions of ice.[59] We expect a similar enhancement in triplet concentrations in aerosol liquid water compared to fog, as a consequence of higher concentrations of brown carbon in water-containing particles relative to fog; in contrast, there should be essentially no change in the main triplet sink, dissolved oxygen. While the extent of this enhancement needs to be studied under atmospherically relevant concentrations, it is very likely that laboratory studies which employ very high concentrations of particulate triplet precursors are overestimating the importance of triplet-sensitized oxidation pathways. Similar to triplets, studies in ice have shown enormous enhancements, up to 10^4, in $^1O_2^*$ concentrations relative to the same sample studied as solution due to an increase in the concentration of sources (CDOM) but not sinks (liquid water).[60] For similar reasons we expect that $^1O_2^*$ concentrations will be higher in particle water compared to in fog. Our recent and current work indicate that singlet molecular oxygen and triplet excited states of DOM can be important oxidants in fog drops, so concentration enhancements in aerosol liquid water suggest that they are even more significant oxidants in particles.

ACKNOWLEDGEMENTS

We thank Harsha Vempati, Franz Ehrenhauser, Amie Hansel, Mickael Vaitilingom and Kalliat T. Valsaraj (Louisiana State University) for fog samples and discussions; Aurelie Marcotte, Youliang Wang, and Pierre Herckes (Arizona State University) for fog samples; and Qi Zhang, Caroline Parworth and Lu Yu (UC Davis) for TOC and IC measurements. This research was funded by the National Science Foundation (AGS-1105049 and AGS-1649212), the California Agricultural Experiment Station (Project CA-D-LAW-6403-RR), a Donald G. Crosby Graduate Fellowship, the UC Davis Graduate Studies Dean's Office, a UC Guru Gobind Singh Fellowship, and the Agricultural and Environmental Chemistry Graduate Group at UC Davis

Tables and Figures

Table 1: Kinetics of triplet excited states of organic matter

Fog Sample ID[a]	Mole Fractions of Best Triplet Matches[b] ^{3}2AN*	^{3}3MAP*	^{3}DMB*	^{3}BP*	$\Sigma[^{3}C_i^*]$[c] (10^{-14} M)	P_{3C^*}[d] (μM h^{-1})	Φ_{3C^*}[e] (%)	$\frac{\Phi_{3C^*}}{(\Phi_{1O2^*}/f_\Delta)}$[f]	$\frac{\Sigma[^{3}C_i^*]}{[^{1}O_2^*]}$[g]
UCD1	1.00				15 (8)	380 (210)	13 (7)	0.87 (0.63)	0.50 (0.28)
UCD2		0.77	0.23		2.6 (2.0)	66 (53)	1.3 (1.1)	0.20 (0.19)	0.11 (0.10)
UCD3		0.80	0.20		2.9 (1.8)	75 (49)	0.91 (0.58)	0.20 (0.17)	0.11(0.08)
UCD4			0.99	0.01	1.4 (0.7)	37 (20)	0.35 (0.19)	0.17 (0.12)	0.10 (0.05)
LSU1	0.80	0.20			8.9 (6.0)	230 (160)	4.0 (2.8)	0.90 (0.78)	0.52 (0.38)
LSU2			0.92	0.08	0.70 (0.45)	18 (12)	3.3 (2.2)	0.15 (0.12)	0.084 (0.058)
LSU4		0.60	0.40		3.6 (1.3)	93 (38)	2.5 (1.0)	0.44 (0.27)	0.26 (0.10)
Average (± 1σ)					5.0 (5.1)	130 (130)	3.7 (4.5)	0.42 (0.34)	0.24 (0.19)
Median					2.9	75	2.5	0.20	0.11

Uncertainties (in parentheses) are ± 1 standard error (unless otherwise stated), obtained by propagating the errors in each term involved.

[a] Sample LSU3 not shown since none of the model triplets yielded a satisfactory match between $\Sigma[^{3}C_i^*]_{SYR}$ to $\Sigma[^{3}C_i^*]_{MeJA}$ likely because the value for $k'_{SYR,3C^*}$ was not statistically different from zero (Figure S5).

[b] Model triplets whose probe-triplet second-order rate constant ratios most closely match the $k'_{SYR,3C^*}$ / $k'_{MeJA,3C^*}$ ratio in the sample. For UCD1, since there is no model ratio higher than 100, the only designated best triplet match is ^{3}2AN*. Mole fractions (indicated in parentheses) of the best triplet matches are used to calculate mole-fraction-weighted bimolecular rate constants for the fog triplets reacting with the probes i.e., $\chi_{3C1^*} \times k_{Probe+3C1^*} + \chi_{3C2^*} \times k_{Probe+3C2^*}$ using eqs 6 and 7 (Supporting Information section S3).

[c] Best estimate of triplet steady-state concentration calculated as the average of $\Sigma[^{3}C_i^*]_{SYR}$ and $\Sigma[^{3}C_i^*]_{MeJA}$ using eqs 8 and 9 (and Supporting Information section S3).

[d] Rate of photoproduction of oxidizing triplet excited states (eq 10).

[e] Quantum yield for formation of oxidizing organic triplet excited states (eq 11).

[f] Fraction of triplets involved in electron transfer or oxidation reactions, assuming f_Δ = 0.53 (± 0.23) (Table S7). The denominator of this expression is the total quantum yield of all triplets, $\Phi_{3C^*(Total)} = \Phi_{1O2^*}/f_\Delta$; this includes triplets that oxidize organics + those involved only in energy transfer to form $^{1}O_2^*$. Across 7 fog samples, the $\Phi_{3C^*(Total)}$ values range between 2.1 and 23 %.

[g] Ratio of the measured oxidizing triplet concentrations and singlet oxygen concentrations (latter are given in Table S4).

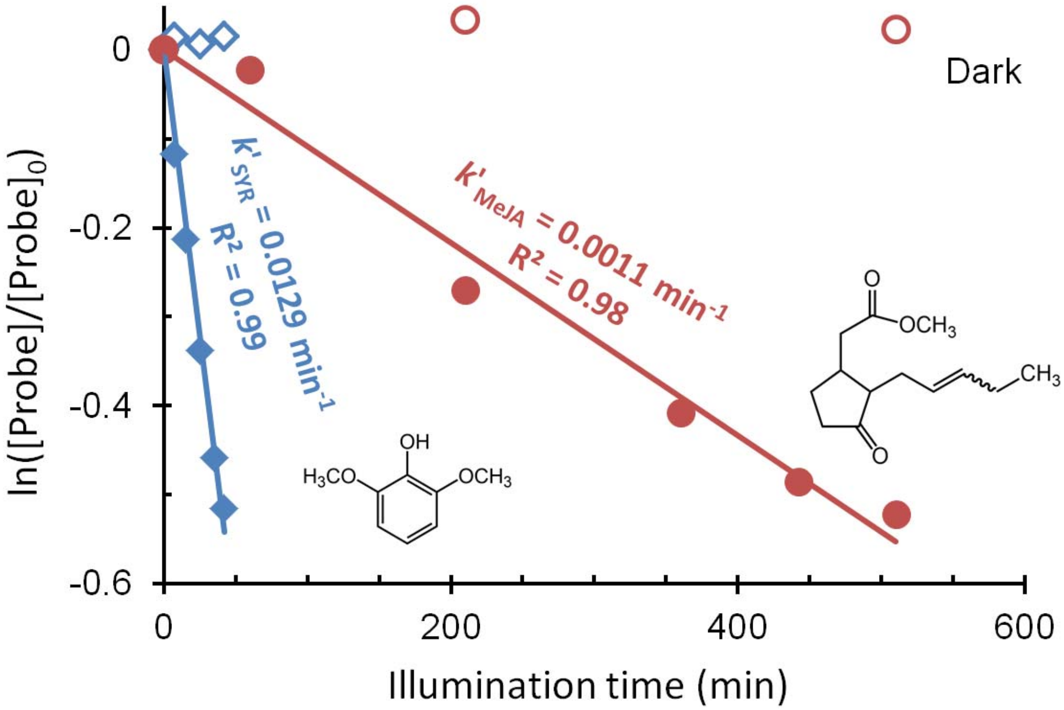

Figure 1: Kinetic measurements of the loss of syringol (blue diamonds) and methyl jasmonate (red circles) in fog sample UCD3. Closed symbols are illuminated samples while open symbols represent dark controls.

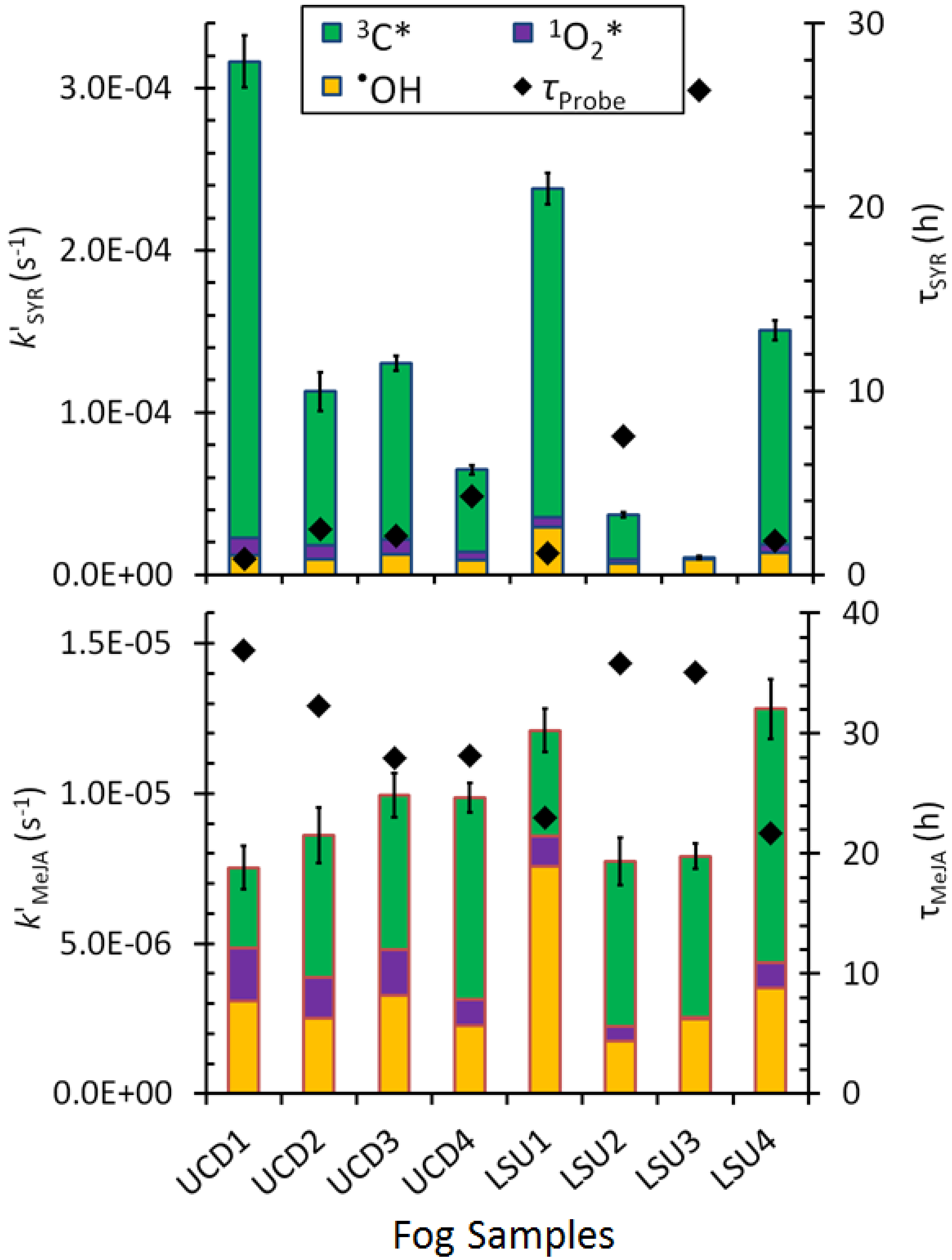

Figure 2: Winter-solstice-normalized pseudo-first-order rate constants (k'_{Probe}) for loss of syringol (top panel) and methyl jasmonate (bottom panel). The bar representing each rate constant is colored to represent the contributions of hydroxyl radical (yellow), singlet molecular oxygen (purple) and triplet excited states (green). The Davis winter lifetime of each probe (τ_{Probe}, black diamonds) is shown on the right y-axes. As described in the methods section, error bars in figures epresent ± 1 standard error, determined by propagating the error from each term involved in calculating the final quantity (i.e., k'_{Probe} here).

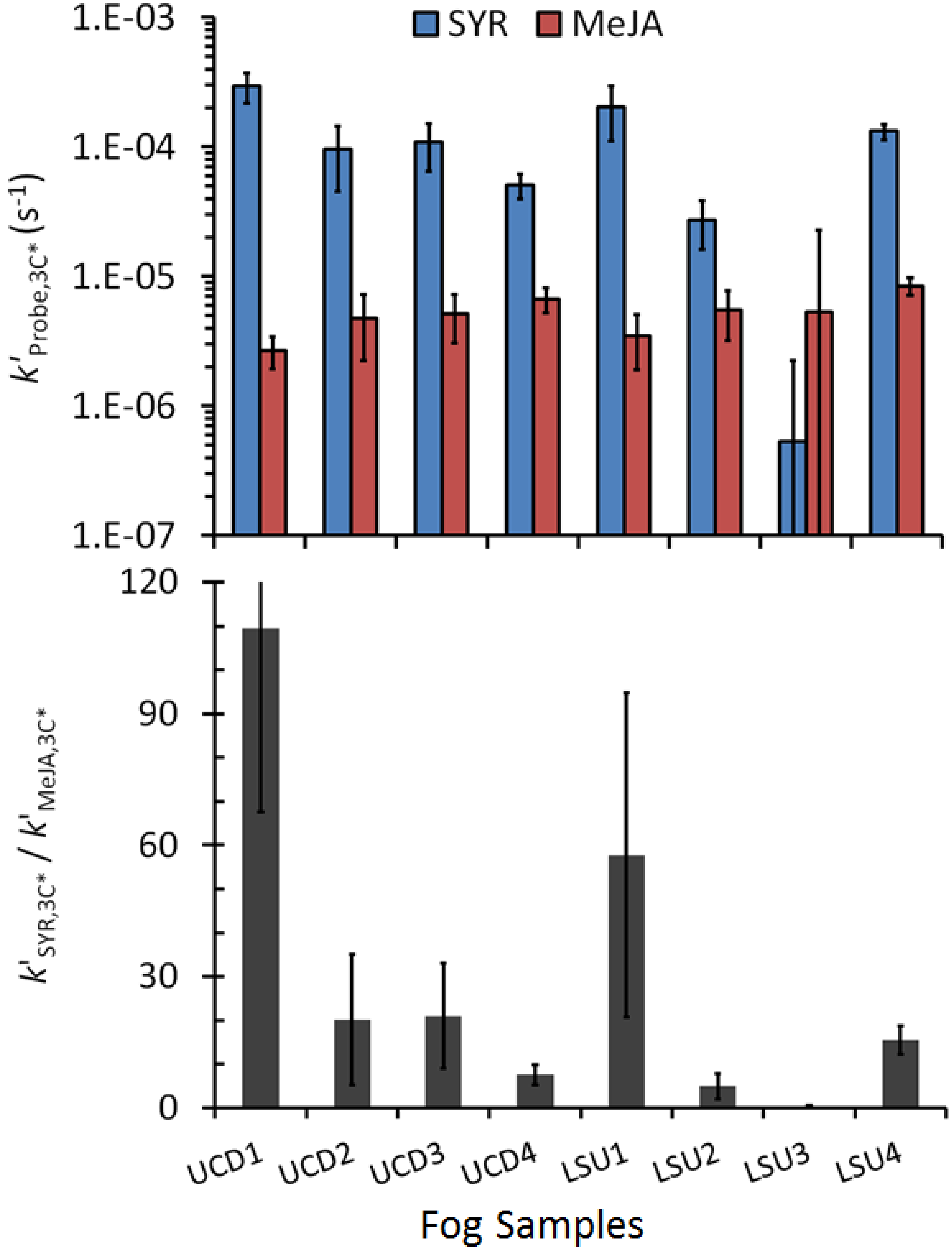

Figure 3: Top panel: Davis winter-solstice-normalized pseudo-first-order rate constants for loss of syringol (blue) and methyl jasmonate (red) due to oxidation by triplet excited states of organic matter. Bottom panel: Ratio of pseudo-first-order rate constants for losses of SYR and MeJA due to triplets. The ratio for sample LSU3 is 0.1 (± 0.5).

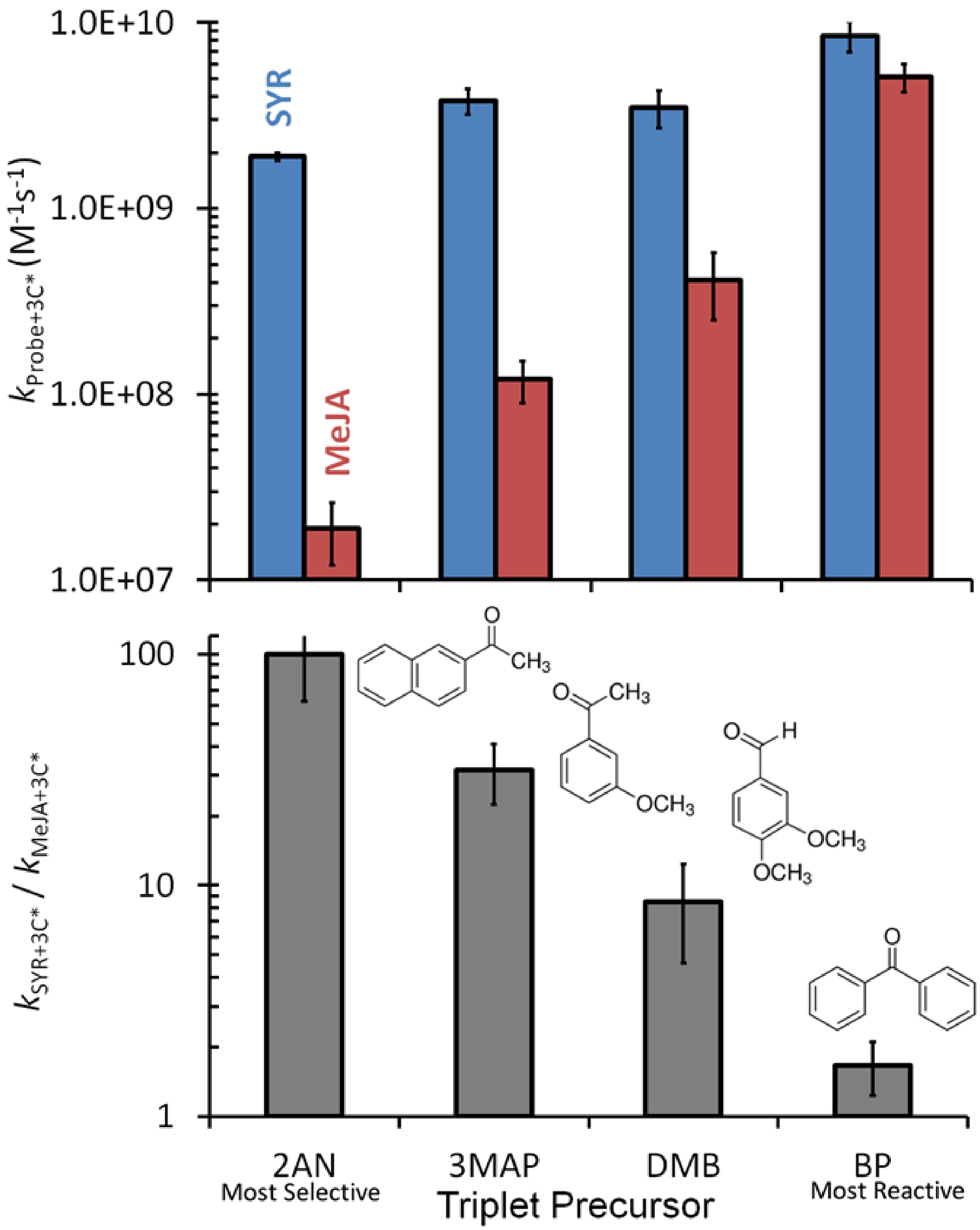

Figure 4: Top panel: Bimolecular rate constants for syringol (blue) and methyl jasmonate (red) with the triplet excited states of four model organics. Values for three of these rate constants are from the literature (SYR + ^{3}DMB*, MeJA + ^{3}DMB*, and MeJA + ^{3}3MAP*),[43, 58] while the other values were measured here (section S1 and Table S6). Bottom panel: Ratio of the bimolecular rate constants for syringol and methyl jasmonate for a given triplet.

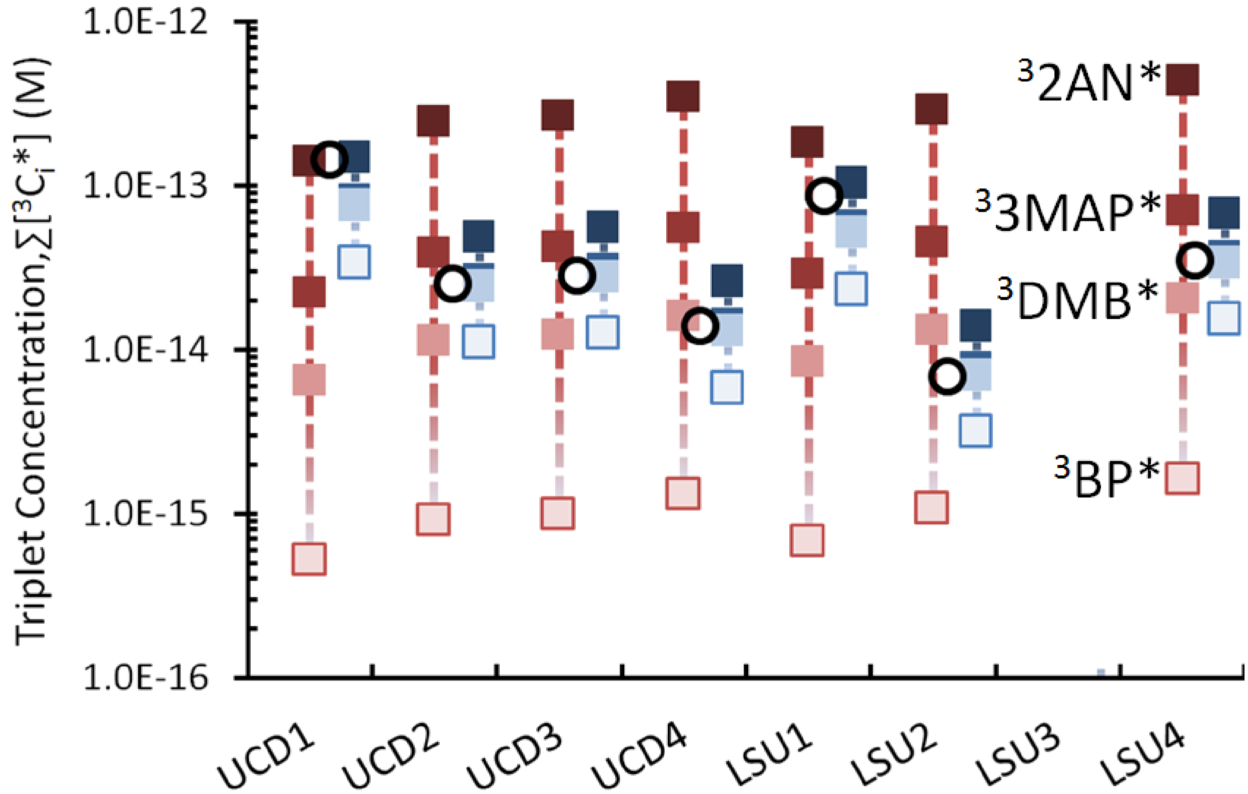

Figure 5: Steady-state concentrations of oxidizing triplet excited states, calculated for each sample using methyl jasmonate (MeJA, red symbols) and syringol (SYR, blue symbols). For a given sample, the vertical line of four red symbols represent the range of triplet concentrations calculated from MeJA loss due to triplets ($k'_{MEJA,3C*}$) and using the four bimolecular rate constants from the model triplet excited states - ^{3}2AN*, ^{3}3MAP*, ^{3}DMB* and ^{3}BP* – in eq 5. The adjacent blue line of symbols represents the corresponding range of triplet concentrations calculated with the syringol decay data and the four model triplets. The best estimate of the overall triplet concentration in each sample lies in the overlapping region and is calculated in the following way: first, one or two model triplets that yield the closest match between the blue and red symbols are identified. Then, the mole-fraction-weighted model rate constants of the best matches are combined (eqs 6 and 7) and used to obtain one triplet concentration each from the SYR and MeJA results (eq 8). These are then averaged to get the best estimate in a given sample (eq 9), which is shown as the black open circle. Sample LSU3 is not shown since there is no match between steady-state concentrations for any model triplet (Table S11, Figure S5), likely because the syringol decay due to triplets is not statistically different from zero (Table S4).

Supporting Information: Additional experimental data, supplemental analyses in 12 tables, 5 figures, 4 sections. Sections include details on: measurement of second-order rate constants for reactions of model triplets with probes; hypothetical scenarios evaluating the two-probe triplet measurement technique; determining the best estimate triplet concentration in the fog waters using the two-probe technique; evaluating potential significance of other oxidants.

REFERENCES

1. Graedel, T. E.; Weschler, C. J., Chemistry within aqueous atmospheric aerosols and raindrops. *Rev. Geophys.*, **1981,** *19*, (4), 505-539.
2. Munger, J. W.; Jacob, D. J.; Waldman, J. M.; Hoffmann, M. R., Fogwater chemistry in an urban atmosphere. *J. Geophys. Res. Oceans*, **1983,** *88*, (Nc9), 5109-5121.
3. Jacob, D. J., Chemistry of OH in remote clouds and its role in the production of formic acid and peroxymonosulfate. *J. Geophys. Res. Atmos.*, **1986,** *91*, (D9), 9807-9826.
4. Blando, J. D.; Turpin, B. J., Secondary organic aerosol formation in cloud and fog droplets: a literature evaluation of plausibility. *Atmos. Environ.*, **2000,** *34*, (10), 1623-1632.
5. Hastings, W. P.; Koehler, C. A.; Bailey, E. L.; De Haan, D. O., Secondary organic aerosol formation by glyoxal hydration and oligomer formation: Humidity effects and equilibrium shifts during analysis. *Environ. Sci. Technol.*, **2005,** *39*, (22), 8728-35.
6. Altieri, K. E.; Carlton, A. G.; Lim, H. J.; Turpin, B. J.; Seitzinger, S. P., Evidence for oligomer formation in clouds: Reactions of isoprene oxidation products. *Environ. Sci. Technol.*, **2006,** *40*, (16), 4956-60.
7. Altieri, K. E.; Seitzinger, S. P.; Carlton, A. G.; Turpin, B. J.; Klein, G. C.; Marshall, A. G., Oligomers formed through in-cloud methylglyoxal reactions: Chemical composition, properties, and mechanisms investigated by ultra-high resolution FT-ICR mass spectrometry. *Atmos. Environ.*, **2008,** *42*, (7), 1476-1490.
8. Dall'Osto, M.; Harrison, R. M.; Coe, H.; Williams, P., Real-time secondary aerosol formation during a fog event in London. *Atmos. Chem. Phys.*, **2009,** *9*, (7), 2459-2469.
9. Ervens, B.; Turpin, B. J.; Weber, R. J., Secondary organic aerosol formation in cloud droplets and aqueous particles (aqSOA): A review of laboratory, field and model studies. *Atmos. Chem. Phys.*, **2011,** *11*, (21), 11069-11102.
10. Zepp, R. G.; Wolfe, N. L.; Baughman, G.; Hollis, R. C., Singlet oxygen in natural waters. *Nature*, **1977,** *267*, (5610), 421-423.
11. Canonica, S.; Jans, U.; Stemmler, K.; Hoigne, J., Transformation kinetics of phenols in water: Photosensitization by dissolved natural organic material and aromatic ketones. *Environ. Sci. Technol.*, **1995,** *29*, (7), 1822-1831.
12. Warren, J. J.; Tronic, T. A.; Mayer, J. M., Thermochemistry of proton-coupled electron transfer reagents and its implications. *Chem. Rev.*, **2010,** *110*, (12), 6961-7001.
13. Erickson, P. R.; Walpen, N.; Guerard, J. J.; Eustis, S. N.; Arey, J. S.; McNeill, K., Controlling factors in the rates of oxidation of anilines and phenols by triplet methylene blue in aqueous solution. *J. Phys. Chem. A*, **2015,** *119*, (13), 3233-3243.
14. Kaur, R.; Anastasio, C., Light absorption and the photoformation of hydroxyl radical and singlet oxygen in fog waters. *Atmos. Environ.*, **2017,** *164*, 387-397.
15. Anastasio, C.; McGregor, K. G., Chemistry of fog waters in California's central valley: 1. In situ photoformation of hydroxyl radical and singlet molecular oxygen. *Atmos. Environ.*, **2001,** *35*, (6), 1079-1089.
16. Faust, B. C.; Allen, J. M., Aqueous-phase photochemical formation of hydroxyl radical in authentic cloudwaters and fogwaters. *Environ. Sci. Technol.*, **1993,** *27*, (6), 1221-1224.

17. Arakaki, T.; Faust, B. C., Sources, sinks, and mechanisms of hydroxyl radical (•OH) photoproduction and consumption in authentic acidic continental cloud waters from Whiteface Mountain, New York: The role of the Fe (R)(R= II, III) photochemical cycle. *J. Geophys. Res. Atmos.*, **1998,** *103*, (D3), 3487-3504.
18. Anastasio, C.; Faust, B. C.; Allen, J. M., Aqueous-Phase Photochemical Formation of Hydrogen-Peroxide in Authentic Cloud Waters. *J. Geophys. Res. Atmos.*, **1994,** *99*, (D4), 8231-8248.
19. Arakaki, T.; Miyake, T.; Shibata, M.; Sakugawa, H., Photochemical formation and scavenging of hydroxyl radical in rain and dew waters. *Nippon Kagaku Kaishi*, **1999**, (5), 335-340.
20. Albinet, A.; Minero, C.; Vione, D., Photochemical generation of reactive species upon irradiation of rainwater: Negligible photoactivity of dissolved organic matter. *Sci. Total Environ.*, **2010,** *408*, (16), 3367-3373.
21. Anastasio, C.; Newberg, J. T., Sources and sinks of hydroxyl radical in sea-salt particles. *J. Geophys. Res.*, **2007,** *112*, (D10), D10306.
22. Zhou, X. L.; Davis, A. J.; Kieber, D. J.; Keene, W. C.; Maben, J. R.; Maring, H.; Dahl, E. E.; Izaguirre, M. A.; Sander, R.; Smoydzyn, L., Photochemical production of hydroxyl radical and hydroperoxides in water extracts of nascent marine aerosols produced by bursting bubbles from Sargasso seawater. *Geophys. Res. Lett.*, **2008,** *35*, (20), L20803.
23. Arakaki, T.; Anastasio, C.; Kuroki, Y.; Nakajima, H.; Okada, K.; Kotani, Y.; Handa, D.; Azechi, S.; Kimura, T.; Tsuhako, A.; Miyagi, Y., A general scavenging rate constant for reaction of hydroxyl radical with organic carbon in atmospheric waters. *Environ. Sci. Technol.*, **2013,** *47*, (15), 8196-203.
24. Anastasio, C.; Jordan, A. L., Photoformation of hydroxyl radical and hydrogen peroxide in aerosol particles from Alert, Nunavut: Implications for aerosol and snowpack chemistry in the Arctic. *Atmos. Environ.*, **2004,** *38*, (8), 1153-1166.
25. Canonica, S.; Hoigné, J., Enhanced oxidation of methoxy phenols at micromolar concentration photosensitized by dissolved natural organic material. *Chemosphere*, **1995,** *30*, (12), 2365-2374.
26. Arnold, W. A., One electron oxidation potential as a predictor of rate constants of N-containing compounds with carbonate radical and triplet excited state organic matter. *Environ. Sci. Process. Impact.*, **2014,** *16*, (4), 832-838.
27. Canonica, S.; Hellrung, B.; Müller, P.; Wirz, J., Aqueous oxidation of phenylurea herbicides by triplet aromatic ketones. *Environ. Sci. Technol.*, **2006,** *40*, (21), 6636-6641.
28. Bahnmüller, S.; von Gunten, U.; Canonica, S., Sunlight-induced transformation of sulfadiazine and sulfamethoxazole in surface waters and wastewater effluents. *Water Res.*, **2014,** *57*, 183-192.
29. Boreen, A. L.; Arnold, W. A.; McNeill, K., Triplet-sensitized photodegradation of sulfa drugs containing six-membered heterocyclic groups: Identification of an SO_2 extrusion photoproduct. *Environ. Sci. Technol.*, **2005,** *39*, (10), 3630-3638.
30. Renard, P.; Reed Harris, A. E.; Rapf, R. J.; Ravier, S.; Demelas, C.; Coulomb, B.; Quivet, E.; Vaida, V.; Monod, A., Aqueous phase oligomerization of methyl vinyl ketone by atmospheric radical reactions. *J. Phys. Chem. C*, **2014,** *118*, (50), 29421-29430.
31. De Haan, D. O.; Tolbert, M. A.; Jimenez, J. L., Atmospheric condensed-phase reactions of glyoxal with methylamine. *Geophys. Res. Lett.*, **2009,** *36*, (11), L11819.
32. Anastasio, C.; Faust, B. C.; Rao, C. J., Aromatic carbonyl compounds as aqueous-phase photochemical sources of hydrogen peroxide in acidic sulfate aerosols, fogs, and clouds. 1. Non-phenolic methoxybenzaldehydes and methoxyacetophenones with reductants (phenols). *Environ. Sci. Technol.*, **1996,** *31*, (1), 218-232.
33. Fu, H.; Ciuraru, R.; Dupart, Y.; Passananti, M.; Tinel, L.; Rossignol, S. p.; Perrier, S.; Donaldson, D. J.; Chen, J.; George, C., Photosensitized production of atmospherically reactive organic compounds at the air/aqueous interface. *J. Am. Chem. Soc.*, **2015,** *137*, (26), 8348-8351.
34. Rossignol, S.; Tinel, L.; Bianco, A.; Passananti, M.; Brigante, M.; Donaldson, D. J.; George, C., Atmospheric photochemistry at a fatty acid–coated air-water interface. *Science*, **2016,** *353*, (6300), 699-702.

35. Aregahegn, K. Z.; Nozière, B.; George, C., Organic aerosol formation photo-enhanced by the formation of secondary photosensitizers in aerosols. *Faraday Discuss.*, **2013,** *165*, 123-134.
36. Rossignol, S. p.; Aregahegn, K. Z.; Tinel, L.; Fine, L.; Nozière, B.; George, C., Glyoxal induced atmospheric photosensitized chemistry leading to organic aerosol growth. *Environ. Sci. Technol.*, **2014,** *48*, (6), 3218-3227.
37. Tsui, W. G.; Rao, Y.; Dai, H.-L.; McNeill, V. F., Modeling photosensitized secondary organic aerosol formation in laboratory and ambient aerosols. *Environ. Sci. Technol.*, **2017,** *51*, (13), 7496-7501.
38. McNeill, K.; Canonica, S., Triplet state dissolved organic matter in aquatic photochemistry: Reaction mechanisms, substrate scope, and photophysical properties. *Environ. Sci. Process. Impact.*, **2016,** *18*, (11), 1381-1399.
39. Yu, L.; Smith, J.; Laskin, A.; Anastasio, C.; Laskin, J.; Zhang, Q., Chemical characterization of SOA formed from aqueous-phase reactions of phenols with the triplet excited state of carbonyl and hydroxyl radical. *Atmos. Chem. Phys.*, **2014,** *14*, (24), 13801-13816.
40. Ge, X.; Shaw, S. L.; Zhang, Q., Toward Understanding Amines and their Degradation Products from Postcombustion CO_2 Capture Processes with Aerosol Mass Spectrometry. *Environ. Sci. Technol.*, **2014,** *48*, (9), 5066-5075.
41. Galbavy, E. S.; Ram, K.; Anastasio, C., 2-Nitrobenzaldehyde as a chemical actinometer for solution and ice photochemistry. *J. Photochem. Photobiol., A*, **2010,** *209*, (2-3), 186-192.
42. Canonica, S.; Hellrung, B.; Wirz, J., Oxidation of phenols by triplet aromatic ketones in aqueous solution. *J. Phys. Chem. A*, **2000,** *104*, (6), 1226-1232.
43. Richards-Henderson, N. K.; Pham, A. T.; Kirk, B. B.; Anastasio, C., Secondary organic aerosol from aqueous reactions of green leaf volatiles with organic triplet excited states and singlet molecular oxygen. *Environ. Sci. Technol.*, **2014,** *49*, (1), 268-276.
44. Smith, J. D.; Sio, V.; Yu, L.; Zhang, Q.; Anastasio, C., Secondary organic aerosol production from aqueous reactions of atmospheric phenols with an organic triplet excited state. *Environ. Sci. Technol.*, **2014,** *48*, (2), 1049-1057.
45. Finlayson-Pitts, B. J.; Pitts Jr, J. N., *Chemistry of the upper and lower atmosphere: Theory, experiments, and applications*. Academic press: 1999.
46. Halladja, S.; Ter Halle, A.; Aguer, J.-P.; Boulkamh, A.; Richard, C., Inhibition of humic substances mediated photooxygenation of furfuryl alcohol by 2, 4, 6-trimethylphenol. Evidence for reactivity of the phenol with humic triplet excited states. *Environ. Sci. Technol.*, **2007,** *41*, (17), 6066-6073.
47. Golanoski, K. S.; Fang, S.; Del Vecchio, R.; Blough, N. V., Investigating the mechanism of phenol photooxidation by humic substances. *Environ. Sci. Technol.*, **2012,** *46*, (7), 3912-3920.
48. Zepp, R. G.; Schlotzhauer, P. F.; Sink, R. M., Photosensitized transformations involving electronic energy transfer in natural waters: role of humic substances. *Environ. Sci. Technol.*, **1985,** *19*, (1), 74-81.
49. Grebel, J. E.; Pignatello, J. J.; Mitch, W. A., Sorbic acid as a quantitative probe for the formation, scavenging and steady-state concentrations of the triplet-excited state of organic compounds. *Water Res.*, **2011,** *45*, (19), 6535-6544.
50. Sharpless, C. M., Lifetimes of triplet dissolved natural organic matter (DOM) and the effect of $NaBH_4$ reduction on singlet oxygen quantum yields: Implications for DOM photophysics. *Environ. Sci. Technol.*, **2012,** *46*, (8), 4466-4473.
51. Bruccoleri, A.; Pant, B. C.; Sharma, D. K.; Langford, C. H., Evaluation of primary photoproduct quantum yields in fulvic acid. *Environ. Sci. Technol.*, **1993,** *27*, (5), 889-894.
52. Wilkinson, F.; Helman, W. P.; Ross, A. B., Quantum yields for the photosensitized formation of the lowest electronically excited singlet state of molecular oxygen in solution. *J. Phys. Chem. Ref. Data*, **1993,** *22*, (1), 113-262.
53. Canonica, S., Oxidation of aquatic organic contaminants induced by excited triplet states. *CHIMIA*, **2007,** *61*, (10), 641-644.

54. Zepp, R. G.; Wolfe, N. L.; Baughman, G. L.; Hollis, R. C., Singlet oxygen in natural waters. *Nature*, **1977,** *267*, (5610), 421-423.
55. Haag, W. R.; Hoigné, J., Singlet oxygen in surface waters .3. Photochemical formation and steady-state concentrations in various types of waters. *Environ. Sci. Technol.*, **1986,** *20*, (4), 341-348.
56. Haag, W. R.; Gassman, E., Singlet oxygen in surface waters—part I: Furfuryl alcohol as a trapping agent. *Chemosphere*, **1984,** *13*, (5), 631-640.
57. Tratnyek, P. G.; Hoigne, J., Oxidation of substituted phenols in the environment: A QSAR analysis of rate constants for reaction with singlet oxygen. *Environ. Sci. Technol.*, **1991,** *25*, (9), 1596-1604.
58. Smith, J. D.; Kinney, H.; Anastasio, C., Aqueous Benzene-Diols React with an Organic Triplet Excited State and Hydroxyl Radical to form Secondary Organic Aerosol. *Phys. Chem. Chem. Phys.*, **2015,** *17*, (15), 10227-10237.
59. Chen, Z.; Anastasio, C., Concentrations of a triplet excited state are enhanced in illuminated ice. *Environ. Sci. Process. Impact.*, **2017,** *19*, (1), 12-21.
60. Bower, J. P.; Anastasio, C., Measuring a 10,000-fold enhancement of singlet molecular oxygen ($^1O_2$*) concentration on illuminated ice relative to the corresponding liquid solution. *Atmos. Environ.*, **2013,** *75*, 188-195.

Supporting Information for:

First Measurements of Organic Triplet Excited States in Atmospheric Waters

R. Kaur[†,‡] and C. Anastasio[†,‡,*]

[†]Department of Land, Air and Water Resources, University of California-Davis, One Shields Avenue, Davis, CA 95616-8627, USA
[‡]Agricultural and Environmental Chemistry Graduate Group, University of California-Davis, One Shields Avenue, Davis, CA 95616-8627, USA

Correspondence to: C. Anastasio (canastasio@ucdavis.edu)

This supporting information contains: 29 Pages, 12 Tables, 5 Figures, and 4 Sections

Table S1: Fog collection and composition data

Sample ID	Collection Date	Collection Time	pH	DOC µM-C	α_{313} cm^{-1}	[NO_2^-] µM	[NO_3^-] µM	[Cl^-] µM	[SO_4^{2-}] µM	[$HCOO^-$] µM	[NH_4^+] µM	[Ca^{2+}] µM	[Mg^{2+}] µM	[K^+] µM
Fog Samples														
UCD1	01/06/11	05:20-09:50	7.0	607	0.034	12.6	284	4.0	17.3	2.2	397	3.2	0.9	2.4
UCD2	01/15/11	17:30-20:20	5.1	950	0.056	1.1	1070	26.9	90.0	5.1	864	3.6	1.4	2.6
UCD3	01/15/11	23:57-07:25	5.3	1620	0.102	0.02	1830	33.6	211	8.5	1530	4.3	1.2	2.7
UCD4[b]	01/16/11, 01/17/11	00:57-05:15 20:57-00:08	5.1	1790	0.114	0.02	1140	27.0	159	4.7	1500	5.8	1.9	6.4
LSU1	10/26/12	05:00-09:15	6.1	756	0.070	21.5	132	85.8	101	0.1	288	64.3	11.8	7.0
LSU2	11/03/12	04:00-08:40	5.7	336	0.012	2.2	116	30.9	26.1	0.1	133	18.0	4.8	3.5
LSU3[b]	02/06/13, 02/08/13	07:47-09:30 03:01-09:30	4.2	739	0.029	0.07	454	46.2	148	0.1	494	48.2	8.5	6.5
LSU4	10/11/13	3:32-08:30	6.3	863	0.043	11.1	279	31.8	97.5	0.0	439	48.9	8.6	9.5
UCD Average (± 1σ)			5.6 (0.8)	1240 (560)	0.076 (0.038)	3.4 (6.1)	1080 (630)	22.9 (13.0)	119.3 (84.1)	5.1 (2.6)	1070 (550)	4.2 (1.1)	1.4 (0.4)	3.5 (1.9)
LSU Average (± 1σ)			5.6 (0.9)	674 (232)	0.038 (0.024)	8.7 (9.8)	245 (158)	48.7 (25.7)	93.4 (50.4)	0.1 (0.0)	338 (162)	44.9 (19.4)	8.4 (2.9)	6.6 (2.5)
Blanks [a]														
UCDBK1	01/06/11	16:21	5.7	141	0.005	< 0.01	0.6	0.9	1.0	0.1	15.8	1.1	0.7	1.6
UCDBK2	11/12/11	15:00	5.8	38	0.003	< 0.01	1.4	0.1	1.0	0.1	14.7	0.4	0.9	0.9
LSUBK1	01/15/14		5.9	4910	0.022	< 0.01	111	128	41.5	< 0.01	91.1	30.3	15.9	9.3
LSUBK2	02/17/14		5.9	368	0.017	0.07	43.6	31.0	22.1	0.1	53.3	28.1	14.0	10.6
UCDMQ[c]	07/03/14		5.7	7.4	< 0.001	< 0.01	0.1	0.1	0.6	0.1	12.5	0.9	0.8	2.6

[a]Field blanks collected by passing Milli-Q water through fog collector.

[b]Composite sample made by combining fog waters collected over a 2-day period.

[c]Milli-Q water not passed through fog collectors.

Lithium concentrations were below the limit of detection (0.1 µM).

Acetate concentrations were below the limit of detection (0.1 µM) in all samples except UCD1, which had a concentration of 1.1 µM.

Table S2: Measured kinetics of hydroxyl radical and singlet oxygen

Sample ID	R_{abs} (300-450 nm)[a]	P_{OH}[b]	τ_{OH}[c]	$10^4 \times \Phi_{OH}$[d]	P_{1O2}[e]	$10^2 \times \Phi_{1O2*}$[f]
	mol-photons $L^{-1}s^{-1}$	μM h^{-1}	μs		μM h^{-1}	
Samples						
UCD1	7.94E-07	1.4 ± 0.2	1.2 ± 0.2	4.9 ± 0.6	234 ± 44	8.2 ± 1.5
UCD2	1.38E-06	0.82 ± 0.11	1.7 ± 0.4	1.6 ± 0.2	179 ± 81	3.6 ± 1.6
UCD3	2.31E-06	1.3 ± 0.1	1.4 ± 0.1	1.5 ± 0.1	202 ± 77	2.4 ± 0.9
UCD4	2.89E-06	1.6 ± 0.1	0.76 ± 0.05	1.5 ± 0.1	118 ± 24	1.1 ± 0.2
LSU1	1.61E-06	2.5 ± 0.5	1.6 ± 0.6	4.3 ± 0.8	135 ± 36	2.3 ± 0.6
LSU2	1.50E-07	0.47 ± 0.06	2.0 ± 0.7	8.7 ± 1.2	66 ± 16	12 ± 3
LSU3	6.22E-07	0.46 ± 0.01	2.9 ± 0.2	2.1 ± 0.1	9 ± 29	0.40 ± 1.30
LSU4	1.05E-06	1.3 ± 0.1	1.5 ± 0.1	3.4 ± 0.1	111 ± 13	2.9 ± 0.3
UCD Average (±σ)	1.8 (± 0.9)E-06	1.3 (0.3)	1.2 (0.4)	2.4 (1.7)	162 (43)	3.8 (3.1)
LSU Average (±σ)	8.6 (± 6.2)E-07	1.2 (1.0)	2.0 (0.6)	4.6 (2.9)	71 (49)	4.5 (5.3)
Overall Average (±σ)	1.4 (± 0.9)E-06	1.2 (0.7)	1.6 (0.6)	3.5 (2.5)	132 (73)	4.2 (4.0)
Blanks						
UCDBK1	2.84E-07	< 0.08	-	-	≤ 4	-
UCDBK2	1.39E-07	< 0.08	-	-	≤ 5	-
LSUBK1	3.70E-07	< 0.13	-	-	≤ 39	-
LSUBK2	2.83E-07	< 0.15	-	-	≤ 49	-

Listed uncertainties are 1 standard error unless otherwise stated.
All measurements listed here are from our previous paper.[1]
[a] Rate of sunlight absorption in the 300-450 nm wavelength range.
[b] Winter solstice-normalized rate of hydroxyl radical photoproduction.
[c] Lifetime of hydroxyl radical.
[d] Apparent quantum yield of hydroxyl radical, calculated as $\Phi_{OH} = P_{OH} / R_{abs}$.
[e] Winter solstice-normalized rate of singlet oxygen photoproduction.
[f] Apparent quantum yield of singlet oxygen, calculated as $\Phi_{1O2} = P_{1O2} / R_{abs}$

Table S3: Measured syringol and methyl jasmonate loss kinetics

Fog Sample ID	k'_{SYR} [a]	k'_{MeJA} [b]	τ_{SYR} [c]	τ_{MeJA} [d]
	10^{-5} s^{-1}	10^{-6} s^{-1}	h	h
Samples				
UCD1	32 ± 2	7.5 ± 0.7	0.88 ± 0.04	37 ± 4
UCD2	11 ± 1	8.6 ± 0.9	2.5 ± 0.3	32 ± 4
UCD3	13 ± 1	9.9 ± 0.7	2.1 ± 0.1	28 ± 2
UCD4	6.5 ± 0.3	9.9 ± 0.5	4.3 ± 0.2	28 ± 1
LSU1	24 ± 1	12 ± 1	1.2 ± 0.1	23 ± 1
LSU2	3.7 ± 0.1	7.7 ± 0.8	7.5 ± 0.3	36 ± 4
LSU3	1.1 ± 0.1	7.9 ± 0.4	26 ± 2	35 ± 2
LSU4	15 ± 1	13 ± 1	1.8 ± 0.1	22 ± 2
UCD Average (± σ)	16 (11)	9.0 (1.2)	2.4 (1.4)	31 (4)
LSU Average (± σ)	11 (10)	10 (3)	9.2 (11.8)	29 (8)
Overall Average (± σ)	13 (11)[e]	9.6 (2.0)[f]	5.8 (8.6)[e]	30 (6)[f]
Blanks[g]				
UCDBK1	1.5 ± 0.3	-	18 ± 4	-
UCDBK2	≤ 0.3	-	≥ 90	-
LSUBK1	≤ 0.3	-	≥ 90	-
LSUBK2	≤ 0.3	-	≥ 90	-

Listed uncertainties are 1 standard error unless otherwise stated.

[a] Winter-solstice-normalized measured pseudo-first-order rate constant for loss of syringol (SYR).

[b] Winter-solstice-normalized measured pseudo-first-order rate constant for loss of methyl jasmonate (MeJA).

[c,d] Lifetime of syringol and methyl jasmonate, calculated as $1/k'_{SYR}$ and $1/k'_{MeJA}$, respectively.

[e,f] When sample LSU3 is excluded due to its large uncertainties, the overall average k'_{SYR} is 15 (± 10) × 10^{-5} s^{-1} and τ_{SYR} is 2.9 (± 2.3) h; the overall average k'_{MeJA} is 9.8 (± 2.0) × 10^{-6} s¯1 and τ_{MeJA} is 29 (± 6) h; discussed in main text.

[g] Blanks were analyzed by adding 2 μM SYR to an aliquot of the blank and illuminating for 50 minutes. 6.4% loss of SYR was observed in UCDBK1. Under 2% loss over 50 minutes was observed in all other blanks, which was used to calculate an upper limit for k'_{SYR}

Table S4: Syringol loss due to measured photooxidants

Sample ID	[$^{\bullet}$OH] [a]	[$^1O_2$*] [b]	$k'_{SYR,OH}$ [c]	$k'_{SYR,1O2}$ [d]	$k'_{SYR,3C*}$ [e]	$f_{SYR,3C*}$ [f]
	10^{-16} M	10^{-13} M	10^{-5} s^{-1}	10^{-5} s^{-1}	10^{-5} s^{-1}	
Samples						
UCD1	4.6 ± 0.8	3.0 ± 0.6	1.2 ± 0.2	1.1 ± 0.2	29 ± 8	0.93 ± 0.25
UCD2	3.7 ± 0.9	2.3 ± 1.0	0.97 ± 0.24	0.82 ± 0.37	9.5 ± 5.0	0.84 ± 0.44
UCD3	4.9 ± 0.5	2.5 ± 1.0	1.3 ± 0.1	0.92 ± 0.35	11 ± 4	0.83 ± 0.33
UCD4	3.4 ± 0.2	1.5 ± 0.3	0.88 ± 0.06	0.54 ± 0.11	5.1 ± 1.1	0.78 ± 0.17
LSU1	11 ± 4	1.7 ± 0.5	2.9 ± 1.1	0.62 ± 0.17	20 ± 9	0.85 ± 0.38
LSU2	2.6 ± 0.8	0.83 ± 0.21	0.67 ± 0.21	0.30 ± 0.08	2.7 ± 1.1	0.74 ± 0.30
LSU3	3.7 ± 0.3	0.11 ± 0.37	0.96 ± 0.06	0.041 ± 0.133	0.053 ± 0.17	0.05 ± 0.16
LSU4	5.2 ± 0.3	1.4 ± 0.2	1.4 ± 0.1	0.51 ± 0.006	13 ± 2	0.88 ± 0.12
UCD Average (± σ)	4.2 (0.7)	2.3 (0.6)	1.1 (0.2)	0.83 (0.22)	14 (11)	0.85 (0.06)
LSU Average (± σ)	5.7 (3.9)	1.0 (0.7)	1.5 (1.0)	0.37 (0.25)	9.1 (9.4)	0.63 (0.39)
Overall Average (± σ)	4.9 (2.7)	1.7 (0.9)	1.3 (0.7)	0.60 (0.33)	11 (10)[h]	0.74 (0.28)[i]

Listed uncertainties are 1 standard error unless otherwise stated.

[a] Winter-solstice-normalized steady-state concentration of hydroxyl radical measured using benzene as probe.[1]

[b] Winter-solstice-normalized steady-state concentration of singlet oxygen measured using furfuryl alcohol as probe. [1]

[c] Pseudo-first-order rate constant for loss of SYR due to hydroxyl radical, calculated as $k'_{SYR,OH} = k_{SYR+OH} \times [^{\bullet}OH]$.

[d] Pseudo-first-order rate constant for loss of SYR due to singlet oxygen, calculated as $k'_{SYR,1O2} = k_{SYR+1O2} \times [^1O_2^*]$.

[e] Pseudo-first-order rate constant for loss of SYR due to triplet excited states, calculated as $k'_{SYR} - (k'_{SYR,OH} + k'_{SYR,1O2})$.

[f] Fraction of SYR loss due to triplets, calculated as $k'_{SYR,3C*} / k'_{SYR}$; discussed in main text.

[h] When sample LSU3 is excluded due to its large uncertainties, the overall average $k'_{SYR,3C*}$ is 13 (± 9) × 10^{-5} s^{-1}; discussed in main text.

[i] When sample LSU3 is excluded due to its large uncertainties, the overall average $f_{SYR,3C*}$ is 0.84 (± 0.06); discussed in main text.

Table S5: Methyl jasmonate loss due to measured photooxidants

Sample ID	$k'_{MeJA,OH}$ [a]	$k'_{MeJA,1O2}$ [b]	$k'_{MeJA,3C*}$ [c]	$f_{MeJA,3C}$ [d]
	10^{-6} s^{-1}	10^{-6} s^{-1}	10^{-6} s^{-1}	
UCD1	3.1 ± 0.6	1.8 ± 0.3	2.7 ± 0.7	0.36 ± 0.10
UCD2	2.5 ± 0.6	1.4 ± 0.6	4.7 ± 2.5	0.55 ± 0.29
UCD3	3.3 ± 0.3	1.5 ± 0.6	5.2 ± 2.1	0.52 ± 0.21
UCD4	2.3 ± 0.1	0.89 ± 0.18	6.7 ± 1.5	0.68 ± 0.15
LSU1	7.6 ± 2.7	1.0 ± 0.3	3.5 ± 1.6	0.29 ± 0.13
LSU2	1.7 ± 0.6	0.50 ± 0.12	5.5 ± 2.3	0.71 ± 0.30
LSU3	2.5 ± 0.2	0.068 ± 0.22	5 ± 18	0.68 ± 2.22
LSU4	3.5 ± 0.2	0.84 ± 0.01	8.5 ± 1.3	0.66 ± 0.10
UCD Average (± σ)	2.8 (0.5)	1.4 (0.4)	4.8 (1.7)	0.53 (0.13)
LSU Average (± σ)	3.8 (2.6)	0.61 (0.42)	5.7 (2.0)	0.58 (0.20)
Overall Average (± σ)	3.3 (1.8)	1.0 (0.6)	5.3 (1.8)[f]	0.56 (0.16)[g]

Listed uncertainties are 1 standard error unless otherwise stated.

[a] Pseudo-first-order rate constant for loss of MeJA due to hydroxyl radical, calculated as $k'_{MeJA,OH} = k_{MeJA+OH} \times [^{\bullet}OH]$.

[b] Pseudo-first-order rate constant for loss of MeJA due to singlet oxygen, calculated as $k'_{MeJA,1O2} = k_{MeJA+1O2} \times [^{1}O_2*]$.

[c] Pseudo-first-order rate constant for loss of MeJA due to triplet excited states, calculated as $k'_{MeJA} - (k'_{MeJA,OH} + k'_{MeJA,1O2})$.

[d] Fraction of MeJA loss due to triplets, calculated as $k'_{MeJA,3C*} / k'_{MeJA}$; discussed in main text.

[f] When sample LSU3 is excluded due to its large uncertainties, the overall average $k'_{MeJA,3C*}$ is 5.3 (± 1.9) × 10^{-6} s^{-1}; discussed in main text.

[g] When sample LSU3 is excluded due to its large uncertainties, the overall average $f_{MeJA,3C*}$ is 0.54 (± 0.16); discussed in main text.

Table S6: Second-order rate constants for reactions of syringol and methyl jasmonate with hydroxyl radical, singlet oxygen, and triplet excited states

Oxidant	$k_{SYR+Oxidant}$ 10^9 $M^{-1}s^{-1}$	Reference	Reference rate constant, $k_{TMP+Oxidant}$ 10^9 $M^{-1}s^{-1}$ [b]	$k_{MeJA+Oxidant}$ 10^8 $M^{-1}s^{-1}$	Reference	Reference rate constant, $k_{PhOH+Oxidant}$ 10^8 $M^{-1}s^{-1}$ [c]	
$^{\bullet}OH$	26	2	n/a	67 (± 3)	3	n/a	
$^1O_2$*	0.0036	4	n/a	0.0060 (± 0.0007)	5	n/a	
Model Triplets (^{3}C*)							$k_{SYR+3C*}$/ $k_{MeJA+3C*}$ [d]
^{3}2AN*	1.9 (± 0.1)	This work[a]	0.72 (± 0.01)[6]	0.19 (± 0.07)	This work[a]	0.33 (± 0.13)[6]	100 (± 37)
^{3}3MAP*	3.8 (± 0.6)	This work[a]	2.6 (± 0.3)[6]	1.2 (± 0.3)	5		32 (± 9)
^{3}DMB*	3.5 (± 0.8)	7	n/a	4.1 (± 1.6)	5	n/a	8.5 (± 3.8)
^{3}BP*	8.5 (± 1.6)	This work[a]	5.1 (± 0.9)[6]	51 (± 9)	This work[a]	39 (± 7)[6]	1.7 (± 0.4)

Listed uncertainties are 1 standard error.

For measurements made in this work, standard errors are propagated from the relative first-order rate constants of the SYR, MeJA and the bimolecular rate constants for reference compounds reacting with the triplets.

[a] Rate constant was measured using the relative rate technique discussed in Section S1.

[b] Syringol (SYR) rate constants measured in this work used 2,4,6-trimethyl phenol (TMP) as the reference compound.

[c] Methyl jasmonate (MeJA) rate constants measured in this work used phenol (PhOH) as the reference compound.

[d] Ratio of the bimolecular rate constants for reaction of model triplets with syringol (SYR) and methyl jasmonate (MeJA).

Table S7: Characteristics of model triplet species

Model Triplet	E_T [a] (kJ mol^{-1})	$E^0*(^3C*/C^{\bullet -})$ [b] (V)	k_{O2+3C*} [c] (10^9) $M^{-1}s^{-1}$	f_Δ [d]
^{3}2AN*	249	1.10	2.5	0.81 (C_6H_6)
^{3}3MAP*	303	1.64	3.3	0.33 (C_6H_6)
^{3}DMB*	298 (benzaldehyde)[e]	-	-	< 0.61 (MeOH) (estimated)[e]
^{3}BP*	288	1.67	2.6	0.35 (C_6H_6)

All values from Canonica et. al.[6] (E_T , $E^0*(^3C*/C^{\bullet -})$, and k_{O2+3C*}) and Wilkinson et. al. (f_Δ)[8]

[a] Triplet state energy ($T_1 \rightarrow S_0$).

[b] One-electron reduction potential for the triplet/triplet radical anion pair.

[c] Bimolecular rate constant for quenching of triplet by molecular O_2. To calculate rates of triplet photoformation (described in the main text), an average (± 1σ) value of 2.8 (± 0.4) × 10^9 $M^{-1}s^{-1}$ is used.

[d] Yield of singlet oxygen from quenching of model triplet species by O_2. The solvent used in the determination is indicated in parentheses. The average value of f_Δ for the model triplets is 0.53 (± 0.23).

[e] Since the E_T and f_Δ values for ^{3}DMB* are not available, values for benzaldehyde[8, 9] are used as estimates. The f_Δ value is an upper-bound estimate.

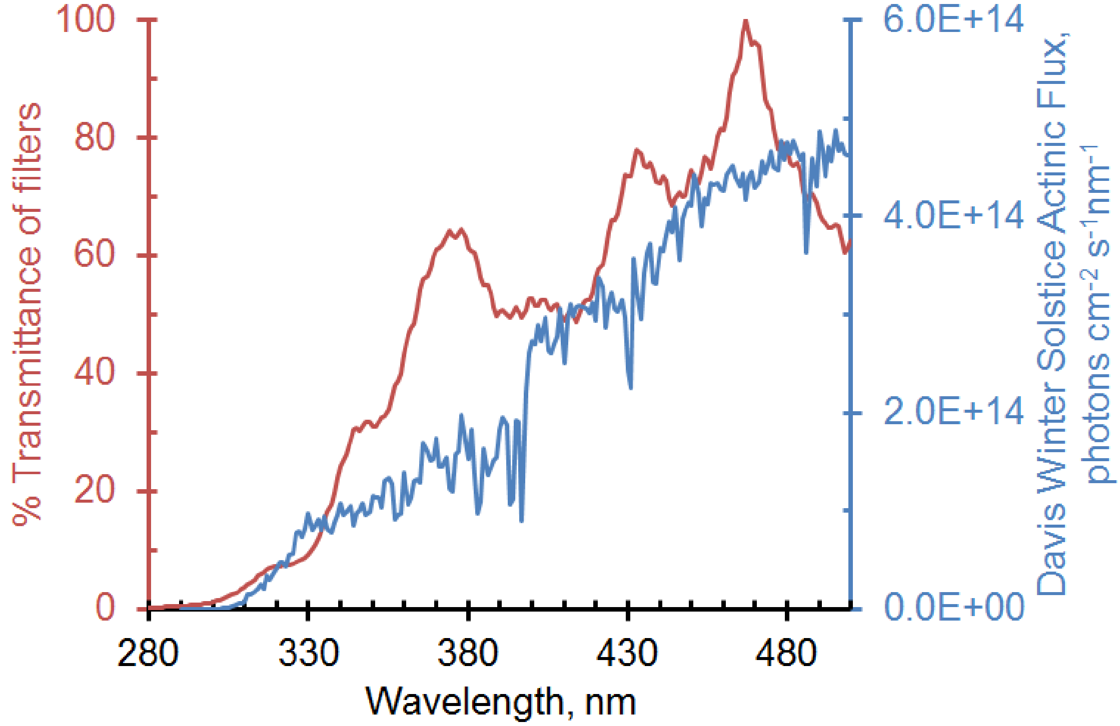

Figure S1: Red line: Measured transmittance of the combination of our two illumination system filters. Blue line: Davis midday, winter solstice actinic flux from the TUV model [10]. Input parameters for the TUV model were: solar zenith angle: 62°, measurement altitude: 0 km, surface albedo: 0.1, aerosol optical depth: 0.235, cloud optical depth: 0.00.

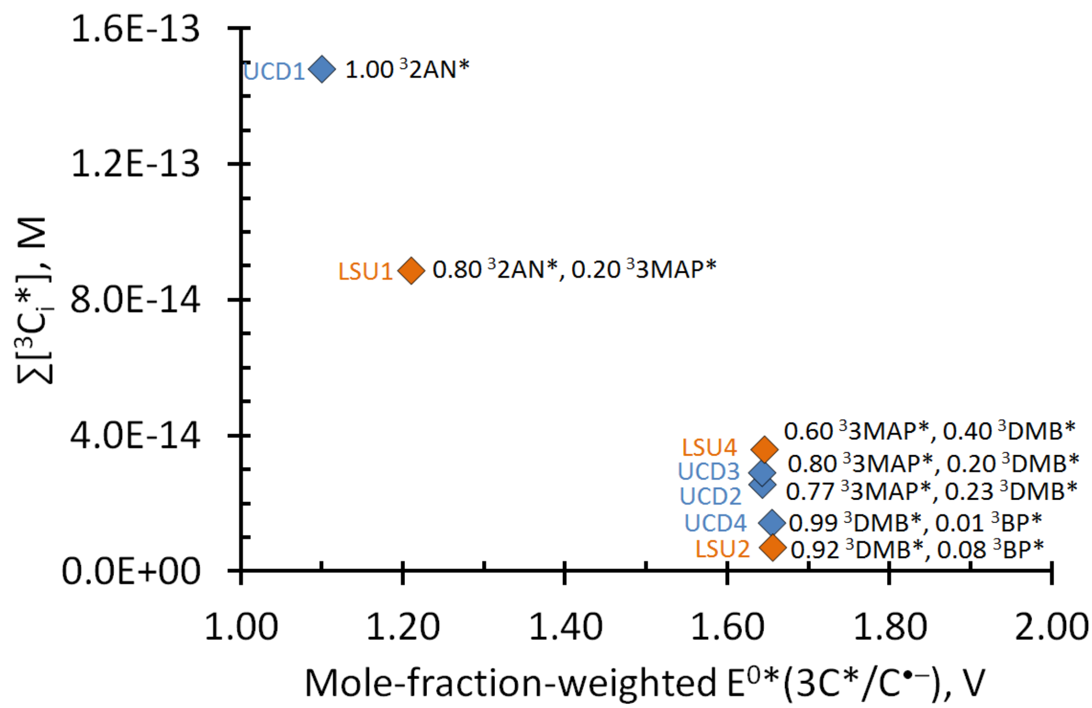

Figure S2: Best estimate triplet steady-state concentration v. mole-fraction-weighted reduction potential of the best triplet matches (values of reduction potential for each model triplet is in Table S7, the mole fractions of best triplet matches in each sample are given in Table S11).

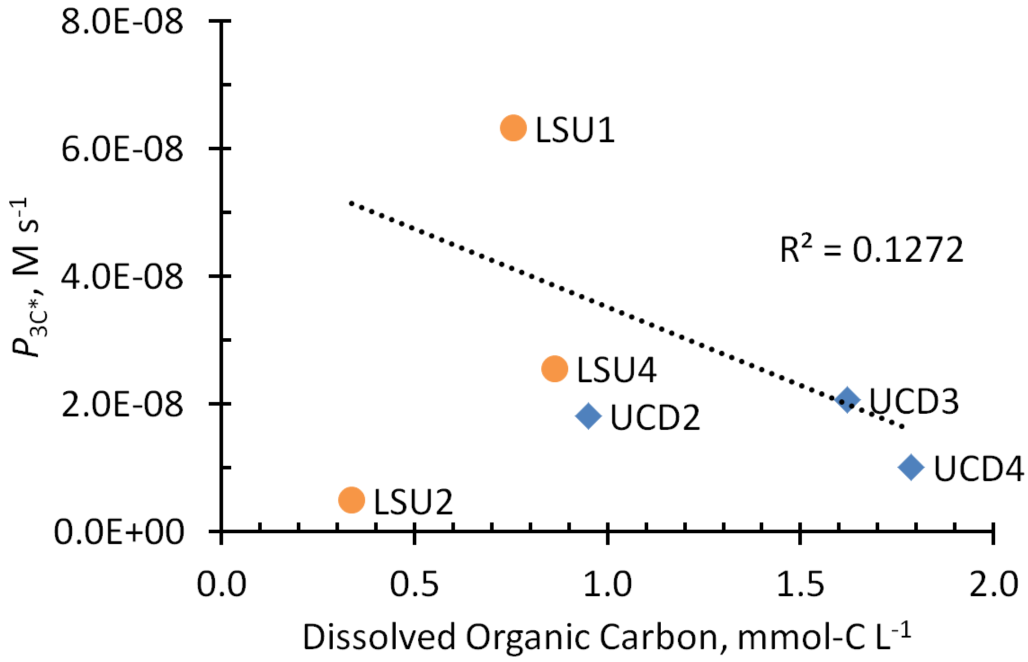

Figure S3: Correlation between the rate of triplet photoproduction (P_{3C^*}) and dissolved organic carbon (DOC) for the Davis, CA (blue diamonds) and Baton Rouge, LA (orange circles) fog samples.

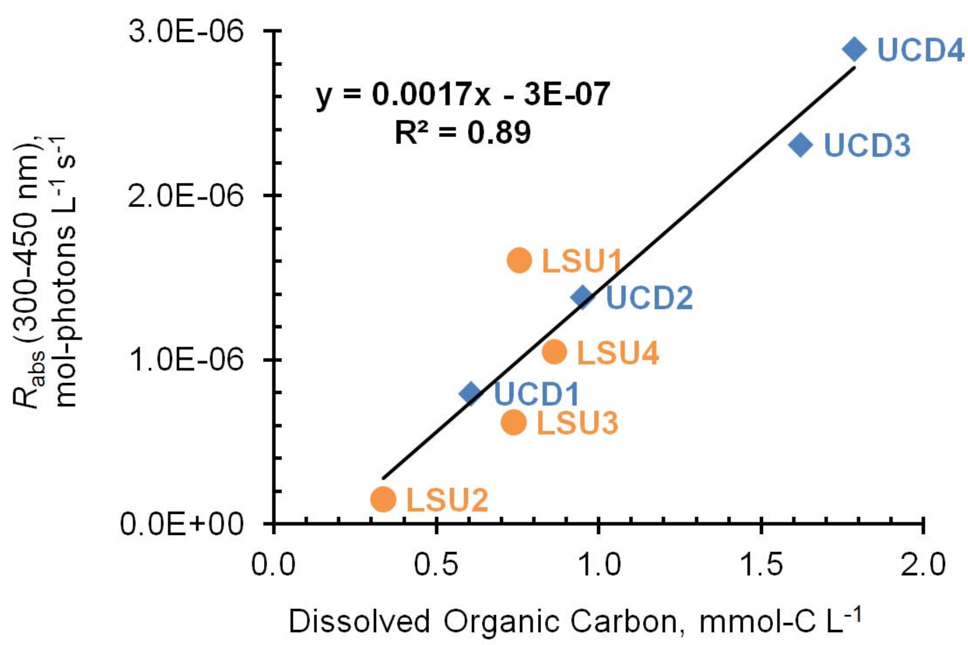

Figure S4: Correlation between the rate of sunlight absorption (R_{abs}) and dissolved organic carbon (DOC) for the Davis, CA (blue diamonds) and Baton Rouge, LA (orange circles) fog samples.

Section S1. Measurement of Second-Order Rate Constants for Model Triplet Precursors

We determined rate constants for the reaction of several triplet excited states with our two triplet probe compounds (syringol and methyl jasmonate) using a relative rate technique.[5, 11] This technique involves illuminating a solution containing a triplet precursor, a reference compound that has a known second-order rate constant with the triplet, and one probe compound for which the rate constant with the triplet is unknown. Air-saturated solutions typically contained 10 µM each of the reference and probe compounds and 20 µM of the triplet precursor. For each experiment, 5 mL of the solution was illuminated in a 1 cm quartz cuvette which was kept capped and stirred continuously. At various intervals, aliquots of the solution were analyzed for the concentration of the reference and probe compounds simultaneously using UV-HPLC. In every case, loss of probe and reference compound followed first-order kinetics. The change in concentration of the probe compound (relative to its starting value) plotted against that of the reference compound (relative to its starting value) yields a linear plot, which is represented by:

$$\ln\frac{[Reference]_0}{[Reference]_t} = \frac{k_{Reference+3C^*}}{k_{Probe+3C^*}} \ln\frac{[Probe]_0}{[Probe]_t} \quad \text{(S1)}$$

where $[\text{Reference}]_0$, $[\text{Reference}]_t$, $[\text{Probe}]_0$, and $[\text{Probe}]_t$ are the concentrations of the reference and probe compounds at time zero and time *t*, respectively, and $k_{\text{Reference+3C*}}$ and $k_{\text{Probe+3C*}}$ are the second-order rate constants for reaction of the reference and probe compounds with the triplet, respectively. A plot of eq S1 (with the y-intercept fixed at the origin) gives a slope equal to $k_{\text{Reference+3C*}} / k_{\text{Probe+3C*}}$; since $k_{\text{Reference+3C*}}$ is known from the literature, the slope is used to calculate $k_{\text{Probe+3C*}}$.

Section S2. Scenarios of Triplet Mixtures to Examine a "Best Estimate" Triplet Concentration in Fog Waters

As discussed in the main text (eq 4), the measured pseudo-first-order rate constant for loss of probe (SYR or MeJA) represents contributions from all of the triplet species *i* in a fog sample:

$$k'_{\text{Probe,3C*}} = (k_{\text{Probe+3C}_1\text{*}} \times [^3\text{C}_1\text{*}]) + (k_{\text{Probe+3C}_2\text{*}} \times [^3\text{C}_2\text{*}]) + (k_{\text{Probe+3C}_3\text{*}} \times [^3\text{C}_3\text{*}]) + \ldots \quad \text{(4, main text)}$$

or

$$k'_{\text{Probe,3C*}} = \Sigma\,(k_{\text{Probe+3Ci*}} \times [^3\text{C}_\text{i}\text{*}]) \quad \text{(S2)}$$

where $k'_{\text{Probe,3C*}}$ is the overall first-order triplet reactivity rate constant (determined by subtracting the contributions of $^{\bullet}$OH and $^1O_2$* from the measured probe loss (eq 3)); $k_{\text{Probe+3Ci*}}$ is the second-order rate constant for each triplet *i* with the probe, and $[^3\text{C}_\text{i}\text{*}]$ is the concentration of each triplet species. Since the identities of the triplet species, and their second-order rate constants with the probes, are unknown in the fog samples, we use data from four model triplets to estimate the triplet steady-state concentration in each sample. Our four model triplet precursors have been previously used in studies of surface or atmospheric waters[12-14]: 2-acetonaphthone (2AN), 3,4-dimethoxybenzaldehyde (DMB), 3'-methoxyacetophenone (3MAP), and benzophenone (BP). The bimolecular reaction rate constants of their triplet excited states with SYR and MeJA span a wide range[5, 6, 14] (Table S6) and thus represent natural triplets with a wide range of reactivity.

We can use the second-order rate constants for the four model triplets reacting with a given probe ($k_{\text{Probe+3C*}}$) to determine a range of four triplet steady-state concentrations in a given fog sample:

$$\Sigma[^3\text{C}_\text{i}\text{*}]_{\text{Probe}} \approx \frac{k'_{\text{Probe,3C*}}}{k_{\text{Probe+3C*}}} = \frac{\Sigma_\text{i}(k_{\text{Probe+3Ci*}} \times [\text{3Ci*}])}{k_{\text{Probe+3C*}}} \quad \text{(S3)}$$

We then repeat the same procedure with the results from the other probe to get a separate range of triplet steady-state concentrations in that sample. Since the triplet steady-state concentration in any sample should be the same irrespective of the probe used for measurement, the true triplet-steady-state concentration should lie within the overlapping portion of the concentration ranges calculated from the two probes in a given sample. Ideally, the two probes should give the same triplet concentration in a sample, i.e.,

$$\sum[^3C_i^*]_{SYR} = \sum[^3C_i^*]_{MeJA} \qquad \text{(S4)}$$

From eqs S3 and S4, it follows:

$$\frac{k'_{SYR,3C^*}}{k_{SYR+3C^*}} = \frac{k'_{MeJA,3C^*}}{k_{MeJA+3C^*}} \qquad \text{(S5)}$$

which can be rearranged as

$$\frac{k'_{SYR,3C^*}}{k'_{MeJA,3C^*}} = \frac{k_{SYR+^3C^*}}{k_{MeJA+^3C^*}} \qquad \text{(S6)}$$

Thus, at the "true" steady-state triplet concentration, the ratio of the pseudo-first-order rate constants for loss of the two probes due to triplet species is equal to the ratio of the second-order rate constants of the two probes reacting with one or more model triplets. The ratios of the model triplet rate constants (i.e., $k_{SYR+3C^*}/k_{MeJA+3C^*}$) for ^{3}2AN*, ^{3}3MAP*, ^{3}DMB* and ^{3}BP* are 100, 32, 8.5, and 1.7, respectively (Table S5) and as discussed in the main text, this rate constant ratio indicates the reactivity of the model triplet species. For example, if a triplet is highly reactive (e.g., ^{3}BP*) it reacts at similar rates with both probes and the ratio is closer to unity. In case of more selective (i.e., less reactive) triplets, the reaction rate constants with the two probes differ significantly and the ratio is large, e.g., ^{3}2AN* has a ratio of 100. Thus the $k'_{Probe,3C^*}$ ratio in eq S6 is an indicator of the average reactivity of the triplet mixture in that sample.

For each sample, the $k'_{Probe,3C^*}$ ratio (Figure 3, main text) falls on or between the ratio for two of the model triplets, which we term the "best triplet matches". We then calculate the mole fractions (χ) for the bimolecular rate constants of the two best triplet matches ($^3C_1^*$ and $^3C_2^*$) so that their ratio is equal to the $k'_{Probe,3C^*}$ ratio:

$$\frac{k'_{SYR,3C^*}}{k'_{MeJA,3C^*}} = \frac{\chi_{3C1^*} \times k_{SYR+3C1^*} + \chi_{3C2^*} \times k_{SYR+3C2^*}}{\chi_{3C1^*} \times k_{MeJA+3C1^*} + \chi_{3C2^*} \times k_{MeJA+3C2^*}} \qquad \text{(6, main text)}$$

We then use these two mole-fraction-weighted second-order rate constants (separately) in the denominator in eq S3 to determine $\sum[^3C_i^*]_{SYR}$ and $\sum[^3C_i^*]_{MeJA}$. We take the average of these two concentrations as our best estimate of the total triplet steady-state concentration, $\sum[^3C_i^*]$.

In this section our goal is to understand the strengths and weaknesses of this approach for estimating triplet concentrations in natural samples. To do this, we examine 15 hypothetical scenarios, each with a total triplet concentration of 1×10^{-13} M but with different mole fractions of the four model triplets (Table S8). In each scenario we calculate the pseudo-first-order rate constants ($k'_{Probe,3C*}$) for SYR and MeJA in the hypothetical mixture using eq S2. We then follow the same procedure used for natural samples: (1) calculate the pseudo-first-order rate constant ratio (i.e., $k'_{SYR,3C*} / k'_{MeJA,3C*}$); (2) compare this ratio to the ratios of the second-order rate constants of the four model triplets (i.e., $k_{SYR+3C*} / k_{MeJA+3C*}$) to identify the one or two model triplets whose second-order rate constant ratios are equal or closest to the $k'_{Probe,3C*}$ ratio; (3) use eq 6 to calculate mole-fraction-weighted bimolecular rate constants such that $(\chi_{3C1*} \times k_{SYR+3C1*} + \chi_{3C2*} \times k_{SYR+3C2*}) / (\chi_{3C1*} \times k_{MeJA+3C1*} + \chi_{3C2*} \times k_{MeJA+3C2*})$ matches the $k'_{Probe,3C*}$ ratio, (4) use the mole-fraction-weighted rate constants in the denominator of eq S3 to calculate $\Sigma[^3C_i^*]_{SYR}$ and $\Sigma[^3C_i^*]_{MeJA}$; and (5) take the average of these concentrations as our best estimate of the triplet steady-state concentration in each scenario. Finally, we compare the best estimate concentration with the assumed true value of 1×10^{-13} M.

We start with the simplest scenario (S1), where there is only one triplet species (^{3}DMB*). As shown in Table S8, the $k'_{Probe,3C*}$ ratio is 8.5, which is equal to the model ratio $k_{SYR+3DMB*}/k_{MeJA+3DMB*}$ so we designate ^{3}DMB* as the best triplet match. Using $k_{Probe+3C*}$ in eq S3, we calculate two values of $\Sigma[^3C_i^*]_{Probe}$ (Table S9). In this case, $\Sigma[^3C_i^*]_{SYR} = \Sigma[^3C_i^*]_{MeJA} = 1 \times 10^{-13}$ M, the true value (Table S9).

Table S8: Hypothetical scenarios with various assumed combinations of triplets and the corresponding pseudo-first order rate constants for SYR and MeJA loss. The total triplet concentration in each scenario was fixed at 1×10^{-13} M.

Hypothetical Scenario	Triplet Mole Fractions in Scenario				Calculated pseudo-first-order rate constant, $k'_{\mathrm{Probe,3C*}}$ (s^{-1})		
	^{3}2AN*	^{3}3MAP*	^{3}DMB*	^{3}BP*	SYR	MeJA	Ratio
S1	0	0	1	0	3.5E-04	4.1E-05	8.5
S2	0	0	0.50	0.50	6.0E-04	2.8E-04	2.2
S3	0.50	0	0.50	0	2.7E-04	2.1E-05	12.6
S4	0.50	0	0	0.50	5.2E-04	2.6E-04	2.0
S5	0	0.50	0	0.50	6.2E-04	2.6E-04	2.4
S6	0.33	0.33	0.33	0	3.1E-04	1.8E-05	16.8
S7	0	0.33	0.33	0.33	5.3E-04	1.9E-04	2.8
S8	0.25	0.25	0.25	0.25	4.4E-04	1.4E-04	3.1
S9	0.20	0.35	0.35	0.10	3.8E-04	7.0E-05	5.4
S10	0.10	0.10	0.10	0.70	6.9E-04	3.6E-04	1.9
S11	0.70	0.10	0.10	0.10	2.9E-04	5.8E-05	5.0
S12	0.90	0.033	0.033	0.033	2.2E-04	2.0E-05	10.9
S13	0.97	0.010	0.010	0.010	2.0E-04	7.5E-06	26.8
S14	0.98	0.0067	0.0067	0.0067	2.0E-04	5.6E-06	35.0
S15	0.99	0.0033	0.0033	0.0033	1.9E-04	3.8E-06	51.5

Table S9: Best triplet matches, mole-fraction-weighted rate constants and best estimate triplet steady-state concentration in the hypothetical scenarios.

Hypothetical Scenario	Best Triplet Matches	Best Triplet Match Mole Fractions		Calculated mole-fraction-weighted second-order rate constants (M^{-1} s^{-1}) $\chi_{3C1*} \times k_{Probe+3C1*} + \chi_{3C2*} \times k_{Probe+3C2*}$			$\sum[^3C_i^*]_{SYR}$	$\sum[^3C_i^*]_{MeJA}$	$\sum[^3C_i^*]$[a] Best Estimate	R.S.D (%)
		χ_{3C1*}	χ_{3C2*}	SYR	MeJA	Ratio	(10^{-13} M)			
S1	^{3}DMB*	1	0	3.5E+09	4.1E+08	8.5	1.0	1.0	1.0	0.00
S2	^{3}DMB*,^{3}BP*	0.50	0.50	6.0E+09	2.8E+09	2.2	1.0	1.0	1.0	0.00
S3	^{3}3MAP*,^{3}DMB*	0.42	0.58	3.6E+09	2.9E+08	12.6	0.74	0.74	0.74	0.03
S4	^{3}DMB*, ^{3}BP*	0.41	0.59	6.5E+09	3.2E+09	2.0	0.81	0.81	0.81	0.05
S5	^{3}DMB*, ^{3}BP*	0.58	0.42	5.6E+09	2.4E+09	2.4	1.10	1.11	1.10	0.21
S6	^{3}3MAP*,^{3}DMB*	0.66	0.35	3.7E+09	2.2E+08	16.8	0.830	0.832	0.83	0.17
S7	^{3}DMB*,^{3}BP*	0.71	0.29	4.9E+09	1.8E+09	2.8	1.068	1.072	1.070	0.22
S8	^{3}DMB*,^{3}BP*	0.77	0.23	4.6E+09	1.5E+09	3.1	0.95	0.95	0.95	0.07
S9	^{3}DMB*,^{3}BP*	0.94	0.06	3.8E+09	7.1E+08	5.4	0.99	0.99	0.99	0.06
S10	^{3}DMB*,^{3}BP*	0.30	0.70	7.0E+09	3.7E+09	1.9	0.98	0.98	0.98	0.01
S11	^{3}DMB*,^{3}BP*	0.92	0.08	3.9E+09	7.7E+08	5.0	0.75	0.75	0.75	0.01
S12	^{3}3MAP*,^{3}DMB*	0.28	0.72	3.6E+09	3.3E+08	10.9	0.62	0.62	0.62	0.01
S13	^{3}3MAP*,^{3}DMB*	0.93	0.07	3.8E+09	1.4E+08	26.8	0.53	0.53	0.53	<0.01
S14	^{3}2AN*,^{3}3MAP*	0.25	0.75	3.3E+09	9.5E+07	35.0	0.59	0.59	0.59	<0.01
S15	^{3}2AN*,^{3}3MAP*	0.72	0.28	2.4E+09	4.7E+07	51.5	0.80	0.80	0.80	<0.01

[a] Best estimate of triplet concentration in the hypothetical scenario, determined as the average of the SYR- and MeJA-derived triplet concentrations. The true value is 1×10^{-13} M.

We next consider hypothetical triplet mixtures of equal proportions of 2 different triplet species, first where the triplets are adjacent in the reactivity order (i.e., ^{3}2AN*/^{3}MAP*, ^{3}MAP*/^{3}DMB*, and ^{3}DMB*/^{3}BP*) and then where they are not (i.e., ^{3}2AN*/^{3}DMB*, ^{3}MAP*/^{3}BP* and ^{3}2AN*/^{3}BP*). For example, in scenario S2 with equal amounts of adjacent triplets ^{3}DMB* and ^{3}BP*, the $k'_{\mathrm{Probe,3C*}}$ ratio (2.2; Table S8) lies between the $k'_{\mathrm{Probe+3C*}}$ ratios for ^{3}DMB* and ^{3}BP* (i.e. 8.5 and 1.7, respectively). Mole fractions of 0.50 for ^{3}DMB* and ^{3}BP* are required so that the mole-fraction-weighted second-order rate constant ratio i.e., $(\chi_{3C1*} \times k_{\mathrm{SYR+3C1*}} + \chi_{3C2*} \times k_{\mathrm{SYR+3C2*}}) / (\chi_{3C1*} \times k_{\mathrm{MeJA+3C1*}} + \chi_{3C2*} \times k_{\mathrm{MeJA+3C2*}})$ equals 2.2, giving an exact solution to this simple mixture (and matching the true concentration of 1×10^{-13} M; Table S9). We find similar exact (and correct) results for the two other 50/50 mixtures of adjacent triplets (data not shown).

However, in the case of 50/50 mixtures of non-adjacent triplets (S3 – S5), the results most deviate from the true concentration whenever the least reactive triplet (^{3}2AN*) is present in the binary mixture. For example, in S3, even though the hypothetical mixture contains 50% ^{3}2AN* and 50% ^{3}DMB*, the resulting $k'_{\mathrm{Probe,3C*}}$ ratio of 12.6 indicates that the best triplet matches are ^{3}MAP* and ^{3}DMB* and the best estimate of the triplet concentration is low, at 0.74×10^{-13} M (Table S9). Similarly in S4, which contains 50% ^{3}2AN* and 50% ^{3}BP*, the $k'_{\mathrm{Probe,3C*}}$ ratio is 2.0 giving ^{3}DMB* and ^{3}BP* as the best triplet matches, and the triplet concentration is again lower than the true value at 0.81×10^{-13} M. In both S3 and S4, the more reactive model triplet in the mixture (^{3}DMB* and ^{3}BP*, respectively) has a much faster reaction rate constant than ^{3}2AN*, which skews the $k'_{\mathrm{Probe,3C*}}$ values and their ratio. The resulting low ratios make it appear that the scenarios contain triplets of higher reactivity than they actually do, but the steady-state concentrations are lower to compensate.

We also considered scenarios that are variations of S3 and S4, i.e., binary mixtures containing unequal amounts of ^{3}2AN* and either ^{3}DMB* or ^{3}BP* (not shown). These also resulted in $k'_{\mathrm{Probe,3C*}}$ ratios that indicate higher triplet reactivity and correspondingly low triplet concentration best estimates, but the concentrations always fell within a factor of two of the true value. In scenario S5, which is an equal mixture of ^{3}MAP* and ^{3}BP*, the difference in reactivity of the two model triplets is not as large as the scenarios containing ^{3}2AN*, and the resulting best estimate of the triplet concentration of 1.1×10^{-13} M agrees very well with the true value (Table S9). However, even in this scenario, the $k'_{\mathrm{Probe,3C*}}$ ratio is skewed by the more reactive triplet ^{3}BP and comes out to be 2.4, and thus, the best triplet matches end up being ^{3}DMB* and ^{3}BP*. Herein lies the most important caveat of this approach: since we have only a rough proxy of the reactivity of the triplet mixture (i.e., the $k'_{Probe,3C*}$ ratio), the best triplet matches only represent the "average apparent reactivity" (or mole-fraction-weighted reactivity of the triplet mixture).

Next, we consider ternary scenarios. S6 and S7 each both contain three model triplets, evenly split (Table S8). Scenario S6, which contains the less reactive ^{3}2AN*, has a $k'_{Probe,3C*}$ ratio of 16.8, as compared to the ratio of 2.8 in S7, which contains the more reactive triplet mixture. In both cases, the best triplet matches are again the more reactive ones in the mixture, because their faster rate constants skew the mole-fraction-weighted rate constants, i.e. the $\chi_{3C1*} \times k_{Probe+3C1*} + \chi_{3C2*} \times k_{Probe+3C2*}$ values. Regardless, for both scenarios the best estimate of $\Sigma[^3C_i*]$ is within 20% of the true value (Table S9). Comparing the results of scenarios S6 and S7, it appears once again that the technique performs less well when the mixture contains a large percentage of the less reactive triplet ^{3}2AN*.

We next examine quaternary mixtures of all four of the model triplets, starting with two scenarios with relatively even amounts (scenarios S8 and S9). In both cases, the best triplet matches are (again) the most reactive pair of triplets (^{3}DMB* and ^{3}BP*) and the triplet steady-state concentrations are within 5% of the true value (Table S9). Scenarios S10 and S11 have triplet mixtures that contain a majority fraction of highly reactive or less reactive triplet species, respectively. In S10 (majority highly reactive triplets), there is excellent agreement between the assumed and best estimate $\Sigma[^3C_i*]$; however, we see again that in S11, which consists of majority selective triplet (70% ^{3}2AN*), the best match triplet is too reactive (compared to the hypothetical mixture) and the best estimate of $\Sigma[^3C_i*]$ is only 75% of the true value. In this scenario, the low $k'_{Probe,3C*}$ ratio of 5.0 masks the presence of the less reactive ^{3}2AN*.

To further examine this weakness of the technique, we consider scenarios S12- S15 (Table S8), all of which contain mostly the least reactive triplet, ^{3}2AN*. Going from S12 to S15, the ^{3}2AN* fraction increases from 90 to 99%, causing the $k'_{Probe,3C*}$ ratio to increase five-fold, from 10.9 to 51.5. As the proportion of ^{3}2AN* approaches 100%, the $k'_{Probe,3C*}$ ratio becomes more sensitive to increases in ^{3}2AN*. When the ratio is close to, but just under 32, the best matches are ^{3}3MAP* and ^{3}DMB*; because of this, the mole-fraction-weighted rate constants are large and consequently, the triplet steady-state concentration is underestimated by almost a factor of two. However, in S14 and S15, as the fraction of ^{3}2AN* increases beyond 97%, the $k'_{Probe,3C*}$ ratio goes above 32 and the triplet best matches switch to ^{3}2AN* and ^{3}3MAP*. In all four scenarios (S12 – S15) the best match triplets underestimate the mole fraction of the least reactive triplet (i.e., overestimate the triplet reactivity) but also underestimate the total triplet concentration, as seen in simpler mixtures.

In summary, based on these hypothetical scenarios the best estimate of the total triplet steady-state concentration is: (1) typically within 25% of the true value, (2) is never significantly overestimated, and (3) is underestimated (by up to a factor of two) in cases where low-reactivity triplets constitute the largest mole fraction of the triplet mixture. As for the identification of the best-match triplet identities, our technique identifies the one or two triplets whose reactivity is similar to the average reactivity of the mixture of triplets.

S2.1 Syringol alone as the triplet probe

Finally, we also examine whether syringol alone (after correcting for losses due to $^{\bullet}OH$ and $^{1}O_2^*$) could be used as a triplet probe by examining its utility in the same 15 hypothetical scenarios described above (Table S8).

Starting with eq 3 in the main text, we first correct SYR loss due to $^{\bullet}OH$ and $^{1}O_2^*$

$$k'_{SYR,3C*} = \Sigma(k_{SYR+3Ci*}[^3C_i^*]) = k'_{SYR} - (k_{SYR+OH}[^{\bullet}OH] + k_{SYR+1O2*}[^1O_2^*]) \qquad \text{(3, main text)}$$

We then calculate four values of $\Sigma[^3C_i^*]_{SYR}$ by dividing $k'_{SYR,3C*}$ by each of the four bimolecular rate constants of SYR with the four model triplets, $k_{Probe+3C*}$ (Table S6):

$$\Sigma[^3C_i^*]_{SYR} \approx \frac{k'_{SYR,3C*}}{k_{SYR+3C*}} \qquad \text{(S7)}$$

Then we take an average of the four concentrations as the triplet concentration using only syringol as a probe. As shown in Table S10, simply using SYR as the triplet probe does a fair job of estimating triplet steady-state values, since the four bimolecular rate constants for SYR reacting with the model triplets vary by no more than a factor of 5.

For 14 of the 15 scenarios, the average $\Sigma[^3C_i^*]_{SYR}$ value is within a factor of two of the assumed true value. However, while the average SYR-derived concentration is simpler to determine, our two-probe technique has three advantages: (1) it gives some insight into the apparent reactivity of the triplets in the sample, (2) it rarely overestimates the steady-state triplet concentration, while the syringol-only technique frequently does, and (3) it generally gives a more accurate estimate of the triplet concentration. In terms of this last point, for the 15 scenarios, the average absolute relative percent difference (|calculated-true|/true) × 100%) for the two-probe technique is 17 %, while for the SYR-only technique the average absolute RPD is 42 %.

Table S10: Estimated triplet steady-state concentration from using syringol as the sole probe for the 16 hypothetical scenarios described in Table S8. In each scenario the true triplet concentration is 1 × 10^{-13} M. Listed uncertainties are ±1 standard deviation; the relative standard deviation in each case is 57%, which is the RSD for the average of the four rate constants for SYR with the four model triplets.

Hypothetical Scenario	Average (± σ) $\sum[^3C_i^*]_{SYR}$ (10^{-13} M)	$\frac{\text{Average } \sum[^3C_i^*]_{SYR}}{\text{Best Estimate}}$
S1	1.0 (± 0.6)	1.0
S2	1.8 (± 1.0)	1.8
S3	0.85 (± 0.48)	0.81
S4	1.6 (± 0.9)	1.9
S5	1.1 (± 0.6)	1.8
S6	0.91(± 0.52)	1.1
S7	1.6 (± 0.9)	1.5
S8	1.3 (± 0.8)	1.4
S9	1.1 (± 0.6)	1.1
S10	2.0 (± 1.2)	2.1
S11	0.87 (± 0.49)	1.2
S12	0.67 (± 0.38)	1.1
S13	0.60 (± 0.34)	1.1
S14	0.59 (± 0.33)	1.0
S15	0.58 (± 0.33)	0.73

Section S3. Determining the "Best Estimate" Triplet Concentration in Fog Waters using the two-probe technique

Using the measured loss of both probes (k'_{SYR} and k'_{MeJA}), we obtained a best estimate of the triplet steady-state concentration using essentially the technique described in section S2 for the hypothetical scenarios: starting with the measured pseudo-first-order rate constants for probe loss due to triplets, $k'_{SYR,3C*}$ and $k'_{MeJA,3C*}$ (Tables S4, S5 and Figure 3, main text), we calculated two triplet concentration ranges consisting of eight values using the model bimolecular rate constants in the denominator of the following equation (shown in Figures 4 and 5, main text):

$$\Sigma[^3C_i^*]_{Probe} \approx \frac{k'_{Probe,3C^*}}{k_{Probe+3C_i^*}} \quad \text{(5, main text)}$$

Then, the model triplets which gave the closest match between $k'_{SYR,3C*}$ / $k'_{MeJA,3C*}$ and $k_{SYR+3C*}$ / $k_{MeJA+3C*}$ were designated as the best triplet matches (Table S11). Then, using eq 7 in the main text, we calculated mole-fraction-weighted bimolecular rate constants ($\chi_{3C1*} \times k_{Probe+3C1*} + \chi_{3C2*} \times k_{Probe+3C2*}$) such that their ratio matched the $k'_{Probe,3C*}$ ratio. Using the mole-fraction-weighted rate constants we calculated $\Sigma[^3C_i^*]_{SYR}$ and $\Sigma[^3C_i^*]_{MeJA}$ (eq 8, main text). The average of these is shown as the best estimate triplet steady-state concentration ($\Sigma[^3C_i^*]$) in each scenario (eq 9 and Figure 5, main text; Figure S5). The RSD of these values is similar to the RSD from the best estimate for the hypothetical scenarios (i.e., < 0.1%; Table S11), except for sample UCD1 (6.4%). As a measure of the uncertainty in the value for each sample, we have given the ± 1 standard errors for the best estimate of the triplet steady-state concentrations in Table S11 and Table 1 of the main text.

Table S11: Best-estimate steady-state concentrations measured from syringol and methyl jasmonate loss in the fog samples.

Fog Sample	$k'_{SYR,3C*}$ / $k'_{MeJA,3C*}$ [b]	Best Triplet Matches[c]	Mole-fractions of Best Triplet Matches		Calculated mole-fraction-weighted second-order rate constants, $\chi_{3C1*} \times k_{Probe+3C1*} + \chi_{3C2*} \times k_{Probe+3C2*}$ [d]			Triplet Steady-State Concentration (10^{-13} M)			R.S.D (%)[h]
		$^3C_1$*, $^3C_2$*	χ_{3C1*}	χ_{3C2*}	SYR	MeJA	Ratio	$\sum[^3C_i*]_{SYR}$ [e]	$\sum[^3C_i*]_{MeJA}$ [f]	$\sum[^3C_i*]$ Best Estimate[g]	
UCD1	110 (42)	^{3}2AN*	1	0	1.9E+09	1.9E+07	100	1.5	1.4	1.5 (0.8)	6.4
UCD2	20 (15)	^{3}3MAP*, ^{3}DMB*	0.77	0.23	3.7E+09	1.9E+08	20	0.26	0.26	0.26 (0.20)	0.0011
UCD3	21 (12)	^{3}3MAP*, ^{3}DMB*	0.80	0.20	3.7E+09	1.8E+08	21	0.29	0.29	0.29 (0.18)	0.0071
UCD4	7.5 (2.3)	^{3}DMB*, ^{3}BP*	0.99	0.01	3.6E+09	4.7E+08	7.5	0.14	0.14	0.14 (0.07)	0.010
LSU1	58 (37)	^{3}2AN*,^{3}3MAP*	0.80	0.20	2.3E+09	4.0E+07	58	0.89	0.89	0.89 (0.60)	0.00088
LSU2	4.9 (2.9)	^{3}DMB*, ^{3}BP*	0.92	0.08	3.9E+09	7.9E+08	4.9	0.070	0.070	0.070 (0.045)	0.040
LSU3[a]	0.10 (0.46)										
LSU4	16 (3)	^{3}3MAP*, ^{3}DMB*	0.60	0.40	3.7E+09	2.4E+08	16	0.36	0.36	0.36 (0.13)	0.0016

[a] No model triplet yielded a satisfactory match between $\Sigma[^3C_i*]_{SYR}$ to $\Sigma[^3C_i*]_{MeJA}$ for sample LSU3, because the value for $k'_{SYR,3C*}$ was not statistically different from zero.

[b] Ratio of $k'_{Probe,3C*}$ in the fog samples. Uncertainties in parentheses are ± 1 SE propagated from the errors of $k'_{Probe,3C*}$.

[c] Model triplets whose $k_{Probe+3C*}$ ratio lie closest to the $k'_{Probe,3C*}$ ratio in each sample. For UCD1, since there is no model ratio higher than 100, the only designated best triplet match is ^{3}2AN*.

[d] Mole-fraction-weighted bimolecular rate constants for both probes, calculated as $\chi_{3C1*} \times k_{Probe+3C1*} + \chi_{3C2*} \times k_{Probe+3C2*}$. Bimolecular rate constants for the model triplets are given in Table S6.

[e] Triplet steady-state concentration calculated from syringol loss as $k'_{SYR,3C*} / (\chi_{3C1*} \times k_{SYR+3C1*} + \chi_{3C2*} \times k_{SYR+3C2*})$.

[f] Triplet steady-state concentration calculated from methyl jasmonate loss as $k'_{MeJA,3C*} / (\chi_{3C1*} \times k_{MeJA+3C1*} + \chi_{3C2*} \times k_{MeJA+3C2*})$.

[g] Best estimate steady-state concentration calculated as the average of the $\Sigma[^3C_i*]_{SYR}$ and $\Sigma[^3C_i*]_{MeJA}$. The uncertainties shown in parentheses are ± 1 standard error, obtained by propagating standard errors in $k'_{Probe,3C*}$ ratio and the mole-fraction-weighted second-order rate constants.

[h] Relative standard deviation calculated as σ/mean of the $\Sigma[^3C_i*]_{SYR}$ and $\Sigma[^3C_i*]_{MeJA}$ values in each sample.

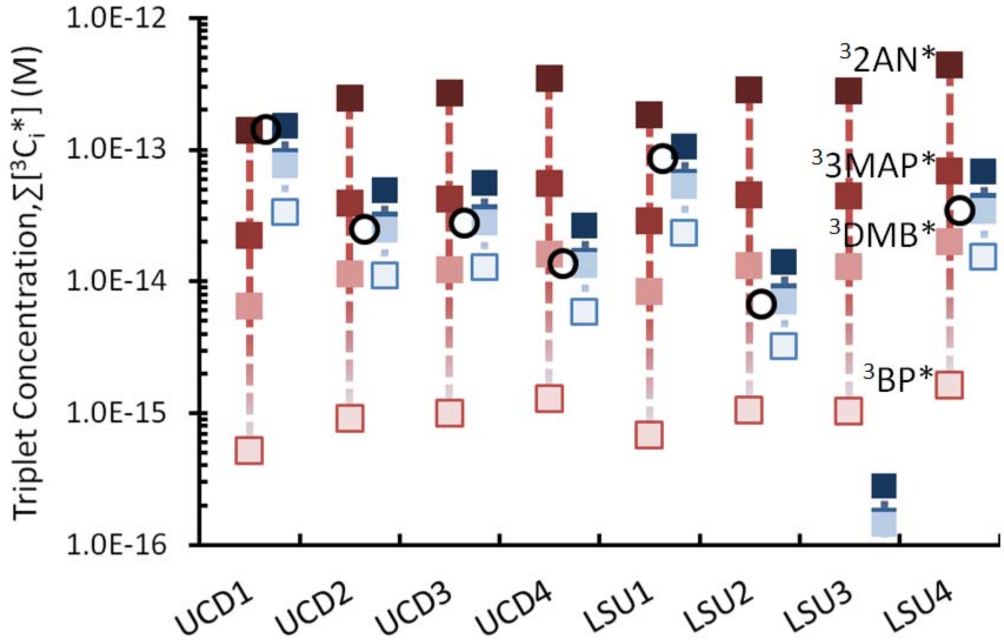

Figure S5: Triplet steady-state concentrations calculated for each fog sample using decay data from syringol (blue) and methyl jasmonate (red) and bimolecular rate constants from the four surrogate triplets**:** ^{3}2AN*, ^{3}3MAP*, ^{3}DMB* and ^{3}BP* (eq 5, main text). The black open circle represents the best estimate of the overall triplet concentration in each sample. Given the divergence in the calculated triplet concentrations in LSU3 between SYR and MeJA, we make no best estimate of concentration.

Since SYR reacts rapidly ($k > 1 \times 10^9$ $M^{-1}s^{-1}$) with all 4 model triplets, averaging the four $\Sigma[^3C_i^*]_{SYR}$ values for each fog sample also yields an estimate of the steady-state triplet concentration for that sample. As shown in Table S12, these SYR-only derived values are statistically similar to the results from the two-probe technique. However, as discussed in section S2, the two-probe technique has a number of advantages over the syringol-only technique, so the two-probe results are what we report in the main text.

Table S12: Estimate of triplet steady-state concentrations in the fog samples using only syringol as the triplet probe.

Fog Sample	$\Sigma[^3C_i^*]_{SYR}$ (10^{-13} M) calculated using 2nd-order rate constant for the triplet state of:				$\Sigma[^3C_i^*]_{SYR}$ [a] (10^{-13} M)	$\Sigma[^3C_i^*]$ Best Estimate [b] (10^{-13} M)
	^{3}2AN*	^{3}3MAP*	^{3}DMB*	^{3}BP*		
UCD1	1.5	0.77	0.84	0.35	0.88 (0.50)	1.5
UCD2	0.50	0.25	0.27	0.11	0.28 (0.16)	0.26
UCD3	0.57	0.29	0.31	0.13	0.32 (0.18)	0.29
UCD4	0.27	0.13	0.14	0.060	0.15 (0.09)	0.14
LSU1	1.1	0.53	0.58	0.24	0.60 (0.34)	0.89
LSU2	0.14	0.072	0.078	0.032	0.081 (0.046)	0.070
LSU4	0.69	0.35	0.38	0.16	0.39 (0.22)	0.36

[a] Estimate of the steady-state triplet concentration in the fog samples, calculated as the average of the four values shown in the table. Uncertainties shown are ± 1 standard deviation.
[b] Best estimate steady-state concentration calculated as the average of the $\Sigma[^3C_i^*]_{SYR}$ and $\Sigma[^3C_i^*]_{MeJA}$ from the two-probe technique (Section S2, Table S11).

Section S4. Potential Significance of Other Oxidants

Since we determine the rate constant for probe loss due to triplets in each sample by difference (eq 3), our triplet results will be sensitive to any contributions from oxidants other than $^{\bullet}OH$, $^{1}O_2^{*}$, and triplets. To investigate whether other oxidants might be significant in the loss of our two probes, here we estimate the potential contributions to probe loss from several other oxidants: hydroperoxyl radical/superoxide radical anion ($HO_2^{\bullet}$/$^{\bullet}O_2^{-}$), ozone (O_3), carbonate radical ($^{\bullet}CO_3^{-}$) and hydrogen ion/hydrated electron ($H^{\bullet}$ (aq)/e^{-}(aq)). Due of a dearth of second-order rate constants for these oxidants with MeJA, we are only able to estimate their contributions to the loss of syringol. In each case, we estimate the pseudo-first-order loss rate constant of syringol due to that oxidant. Then we compare that to the average (± σ) measured pseudo-first order rate constant for syringol loss in 7 fog samples (excluding LSU3) (k'_{SYR} = 1.3 (± 1.0) × 10^{-4} s^{-1}) to determine the likely importance of the oxidant in our fog samples.

Hydroperoxyl Radical / Superoxide Radical Anion (O_2 (-I))

Hydroperoxyl radical and superoxide radical anion (i.e., O_2(-I)) are a conjugate acid-base pair; the pK_a of $HO_2^{\bullet}$ is 4.75 ± 0.08.[15] Since the pH of our fog samples was almost always in the range of 5.1-7.0 (Table S1), $^{\bullet}O_2^{-}$ is the dominant O_2 (-I) species in our samples. There is no rate constant available for reaction of O_2 (-I) with syringol (2,6-dimethoxyphenol) so we use the fastest reported rate constants for reactions of similar compounds in literature. For substituted phenols, the rate constant for reaction of $^{\bullet}O_2^{-}$ with guaiacol (2-methoxyphenol) is 2.5 × 10^{3} $M^{-1}s^{-1}$;[16] for $HO_2^{\bullet}$, the rate constant with catechol (1,2-benzenediol) is 4.7 × 10^{4} $M^{-1}s^{-1}$.[17] Since $HO_2^{\bullet}$ has the higher reaction rate constant, we will consider a fog sample that has the highest proportion of it to obtain an upper bound for the O_2 (-I) contribution to SYR loss. Excluding LSU3, the most acidic sample has a pH of 5.1. At this pH, the mole fractions of $HO_2^{\bullet}$ and $^{\bullet}O_2^{-}$ are 0.31 and 0.69, respectively and the mole-fraction-weighted average rate constant for O_2 (-I) with the SYR proxies is $k_{SYR+O2(-I)}$ = 1.6 × 10^{4} $M^{-1}s^{-1}$.

We estimate the superoxide concentration in our system based on previously measured rates of HOOH formation in illuminated fog waters from California's Central Valley since these two oxidants are intimately connected[18, 19]. The most rapid rate for HOOH formation in the fog waters is likely due to reaction with reduced copper:

$O_2(\text{-I}) + Cu(I) \rightarrow HOOH + Cu(II)$ (S8)

The maximum measured production rate of HOOH, P_{HOOH} , in illuminated Central Valley fogs is 3 μM h^{-1} (8.3×10^{-10} M s^{-1}).[18] The reaction rate constants for both forms of O_2(-I) reacting with Cu(I) are $k_{O_2^- + Cu(I)} = 9.4 \times 10^9$ M^{-1} s^{-1},[20] and $k_{HO2+Cu(I)} = 3.5 \times 10^9$ M^{-1} s^{-1}.[21] At pH 5.1, these rate constants can be combined to give an overall mole-fraction-weighted reaction rate constant, $k_{O2(-I)+Cu(I)}$, of 7.6×10^9 M^{-1} s^{-1}. We assume that the Cu(I) concentration is equal to that of O_2(-I) (as approximately found in the daytime urban cloud scenario of Deguillaume et al.).[19] Solving the rate equation for S8 with these inputs gives an O_2 (-I) steady-state concentration of 3.3×10^{-10} M. Note that this concentration is much lower than modeled values for clouds and fogs because there is negligible partitioning of $HO_2^{\bullet}$ from the gas phase into our sealed containers, in contrast to atmospheric drops. At this concentration, the estimated loss rate constant for syringol due to O_2(-I), $k'_{SYR,O2(-I)}$, is 5.4×10^{-6} s^{-1}, which accounts for 3.6% of the average observed syringol loss. Thus, superoxide is likely a minor sink for syringol in our samples.

Ozone (O_3)

Based on the Henry's law constant for ozone at 25°C ($K_H = 1.1 \times 10^{-2}$ M atm^{-1} [22] and assuming a gas-phase mixing ratio for O_3 of 30 ppbv, we expect an initial aqueous-phase concentration of ozone in our samples of 3.3×10^{-10} M. Like O_2(-I), the actual concentration in our samples is likely lower than this since our samples are capped during illumination. The bimolecular rate constant for reaction of ozone with syringol is not available in the literature, so we assume the rate constant is 10 times faster than the rate constant for O_3 with phenol ($k_{PhOH+O_3} = 1.3 \times 10^3$ M^{-1} s^{-1}) [23], based on the measured ratio of phenol and syringol rate constants for reaction with ^{3}DMB*.[7] Under these assumptions, ozone is also a minor sink for syringol in the fog samples ($k'_{SYR,O_3} = 4.3 \times 10^{-6}$ s^{-1}), accounting for 3% of the average measured syringol loss.

Carbonate Radical ($^{\bullet}CO_3^-$)

The carbonate radical is formed mainly from the reactions of bicarbonate (HCO_3^-) and carbonate (CO_3^{2-}) ions with $^{\bullet}$OH and triplet CDOM species. Although DOM components are likely important sinks for $^{\bullet}CO_3^-$, this quenching is poorly understood.[24-26] Because there are no published measurements of $^{\bullet}CO_3^-$ in atmospheric waters, we use the typical steady-state concentration measured in surface waters, 2 × 10^{-14} M, which was determined using N,N-dimethylaniline as a probe.[26, 27] There are some concerns that use of anilines for measuring $^{\bullet}CO_3^{-}$ overestimates the species since the anilines also react rapidly with triplets,[28] so we expect this is an upper-bound estimate. While $^{\bullet}CO_3^{-}$ reacts rapidly with electron-rich phenoxides (i.e., a phenol that has lost a proton), at fog pH syringol is in the neutral, less reactive, form. There are no rate constants available for $^{\bullet}CO_3^{-}$ reacting with methoxyphenols in the literature. So we assume the rate constant for $^{\bullet}CO_3^{-}$ with SYR is 10 times faster than the value with phenol (k = 4.9 × 10^6 M^{-1} s^{-1} [29]). This gives a pseudo-first-order rate constant for loss of SYR due to carbonate radical, $k'_{SYR,CO3^{\bullet-}}$, of 1 × 10^{-6} s^{-1}. Under these assumptions, $^{\bullet}CO_3^{-}$ is a negligible sink for syringol in the fog samples, accounting for 0.7% of the average measured syringol loss.

Hydrogen Ion / Aquated Electron ($H^{\bullet}_{(aq)}/e^{-}_{(aq)}$)

Hydrogen ion ($H^{\bullet}$) and aquated electron ($e^{-}_{(aq)}$) can be formed during irradiation or illumination of dissolved organic matter in natural waters; these exist as a conjugate acid-base pair with a pK_a of 9.6.[30, 31] In our fog samples, which have an average pH of 5.6, the predominant species would be $H^{\bullet}$ (aq). Zepp and co-workers[32] determined the average steady-state concentration of $e^{-}_{(aq)}$ in sunlight-illuminated lake waters to be 1.2 × 10^{-17} M. As an upper bound, we assume the $H^{\bullet}$ concentration is equal to this. The rate constant for syringol reacting with $H^{\bullet}$ is not known. Using the average rate constant for methoxyphenol, 2.1 × 10^9 $M^{-1}s^{-1}$,[33, 34] , the pseudo-first-order rate constant for loss of SYR due to hydrogen ion, $k'_{SYR, H\bullet}$ is 2.5 × 10^{-8} s^{-1}, which would account for a negligible 0.02 % of the average observed syringol loss.

Combined Contributions from Other Oxidants

Based on our upper-bound estimates, the loss of syringol due to hydroperoxyl radical/superoxide radical anion ($HO_2^{\bullet}/^{\bullet}O_2^{-}$), ozone ($O_3$), carbonate radical ($^{\bullet}CO_3^{-}$) and hydrogen ion/aquated electron ($H^{\bullet}$ (aq)/e-(aq)) combines to ~ 1.0 × 10^{-5} s^{-1}, which is 7.1% of the average measured syringol loss. Based on this, we do not make any corrections for these minor oxidants but assume that the loss of syringol is mainly due to $^{\bullet}OH$, $^1O_2^*$ and $^3C^*$ and that $k'_{Probe,3C*} \approx k'_{SYR} - (k'_{SYR,OH} + k'_{SYR,1O2*})$ (eq 3, main text).

REFERENCES

1. Kaur, R.; Anastasio, C., Light absorption and the photoformation of hydroxyl radical and singlet oxygen in fog waters. *Atmos. Environ.*, **2017,** *164*, 387-397.
2. O'Neill, P.; Steenken, S., Pulse radiolysis and electron spin resonance studies on the formation of phenoxyl radicals by reaction of OH radicals with methoxylated phenols and hydroxybenzoic acids. *Berichte der Bunsengesellschaft für physikalische Chemie*, **1977,** *81*, (6), 550-556.
3. Richards-Henderson, N. K.; Hansel, A. K.; Valsaraj, K. T.; Anastasio, C., Aqueous oxidation of green leaf volatiles by hydroxyl radical as a source of SOA: Kinetics and SOA yields. *Atmos. Environ.*, **2014,** *95*, 105-112.
4. Tratnyek, P. G.; Hoigne, J., Oxidation of substituted phenols in the environment: A QSAR analysis of rate constants for reaction with singlet oxygen. *Environ. Sci. Technol.*, **1991,** *25*, (9), 1596-1604.
5. Richards-Henderson, N. K.; Pham, A. T.; Kirk, B. B.; Anastasio, C., Secondary Organic Aerosol from Aqueous Reactions of Green Leaf Volatiles with Organic Triplet Excited States and Singlet Molecular Oxygen. *Environmental Science & Technology*, **2014,** *49*, (1), 268-276.
6. Canonica, S.; Hellrung, B.; Wirz, J., Oxidation of phenols by triplet aromatic ketones in aqueous solution. *J. Phys. Chem. A*, **2000,** *104*, (6), 1226-1232.
7. Smith, J. D.; Kinney, H.; Anastasio, C., Aqueous benzene-diols react with an organic triplet excited state and hydroxyl radical to form secondary organic aerosol. *Physical Chemistry Chemical Physics*, **2015,** *17*, (15), 10227-10237.
8. Wilkinson, F.; Helman, W. P.; Ross, A. B., Quantum yields for the photosensitized formation of the lowest electronically excited singlet state of molecular oxygen in solution. *J. Phys. Chem. Ref. Data*, **1993,** *22*, (1), 113-262.
9. Hunter, T., Radiationless transition T 1→ S 0 in aromatic ketones. *Transactions of the Faraday Society*, **1970,** *66*, 300-309.
10. Madronich, S., The Tropospheric Visible Ultra-Violet (TUV) model web page. In 2002.
11. Finlayson-Pitts, B. J.; Pitts Jr, J. N., *Chemistry of the upper and lower atmosphere: Theory, experiments, and applications*. Academic press: 1999.
12. Canonica, S.; Hellrung, B.; Müller, P.; Wirz, J., Aqueous oxidation of phenylurea herbicides by triplet aromatic ketones. *Environ. Sci. Technol.*, **2006,** *40*, (21), 6636-6641.
13. Yu, L.; Smith, J.; Laskin, A.; Anastasio, C.; Laskin, J.; Zhang, Q., Chemical characterization of SOA formed from aqueous-phase reactions of phenols with the triplet excited state of carbonyl and hydroxyl radical. *Atmos. Chem. Phys.*, **2014,** *14*, (24), 13801-13816.
14. Smith, J. D.; Sio, V.; Yu, L.; Zhang, Q.; Anastasio, C., Secondary organic aerosol production from aqueous reactions of atmospheric phenols with an organic triplet excited state. *Environmental Science & Technology*, **2014,** *48*, (2), 1049-1057.
15. Bielski, B. H. J.; Cabelli, D. E.; Arudi, R. L.; Ross, A. B., Reactivity of HO_2/O_2^- radicals in aqueous solution. *Journal of Physical and Chemical Reference Data*, **1985,** *14*, (4), 1041-1100.
16. Yasuhisa, T.; Hideki, H.; Muneyoshi, Y., Superoxide radical scavenging activity of phenolic compounds. *International journal of biochemistry*, **1993,** *25*, (4), 491-494.

17. Bielski, B., Evaluation of the reactivities of HO2/O2 with compounds of biological interest. *Oxy Radicals and Their Scavenger Systems. G. Cohen and RA Greenwald (Editors)*, **1983,** *1*, 1-7.
18. Anastasio, C., Aqueous phase photochemical formation of hydrogen peroxide in authentic atmospheric waters and model compound solutions. **1996**.
19. Deguillaume, L.; Leriche, M.; Monod, A.; Chaumerliac, N., The role of transition metal ions on HO_x radicals in clouds: a numerical evaluation of its impact on multiphase chemistry. *Atmos Chem Phys*, **2004,** *4*, (1), 95-110.
20. Piechowski, M. V.; Nauser, T.; Hoignè, J.; Bühler, R. E., O− 2 decay catalyzed by Cu2+ and Cu+ ions in aqueous solutions: a pulse radiolysis study for atmospheric chemistry. *Berichte der Bunsengesellschaft für physikalische Chemie*, **1993,** *97*, (6), 762-771.
21. Berdnikov, V., Catalytic activity of the hydrated copper ion in the decomposition of hydrogen peroxide. *Russ. J. Phys. Chem.*, **1973,** *47*, 1060-1062.
22. Seinfeld, J. H.; Pandis, S. N., *Atmospheric chemistry and physics: From air pollution to climate change*. John Wiley & Sons: 2012.
23. Hoigné, J.; Bader, H., Rate constants of reactions of ozone with organic and inorganic compounds in water—II: Dissociating organic compounds. *Water Res.*, **1983,** *17*, (2), 185-194.
24. Canonica, S.; Kohn, T.; Mac, M.; Real, F. J.; Wirz, J.; von Gunten, U., Photosensitizer method to determine rate constants for the reaction of carbonate radical with organic compounds. *Environmental science & technology*, **2005,** *39*, (23), 9182-9188.
25. Vione, D.; Minella, M.; Maurino, V.; Minero, C., Indirect photochemistry in sunlit surface waters: photoinduced production of reactive transient species. *Chemistry-A European Journal*, **2014,** *20*, (34), 10590-10606.
26. Huang, J.; Mabury, S. A., Steady-state concentrations of carbonate radicals in field waters. *Environmental Toxicology and Chemistry*, **2000,** *19*, (9), 2181-2188.
27. Zeng, T.; Arnold, W. A., Pesticide photolysis in prairie potholes: probing photosensitized processes. *Environmental science & technology*, **2012,** *47*, (13), 6735-6745.
28. Rosario-Ortiz, F. L.; Canonica, S., Probe compounds to assess the photochemical activity of dissolved organic matter. *Environ. Sci. Technol.*, **2016,** *50*, (23), 12532-12547.
29. Chen, S.-N.; Hoffman, M. Z.; Parsons Jr, G. H., Reactivity of the carbonate radical toward aromatic compounds in aqueous solution. *J. Phys. Chem.*, **1975,** *79*, (18), 1911-1912.
30. Kozmér, Z.; Arany, E.; Alapi, T.; Takács, E.; Wojnárovits, L.; Dombi, A., Determination of the rate constant of hydroperoxyl radical reaction with phenol. *Radiat. Phys. Chem.*, **2014,** *102*, 135-138.
31. Buxton, G. V.; Greenstock, C. L.; Helman, W. P.; Ross, A. B., Critical review of rate constants for reactions of hydrated electrons, hydrogen atoms and hydroxyl radicals ($^{\cdot}OH/^{\cdot}O^{-}$) in aqueous solution. *J. Phys. Chem. Ref. Data*, **1988,** *17*, (2), 513-886.
32. Zepp, R. G.; Braun, A. M.; Hoigne, J.; Leenheer, J. A., Photoproduction of hydrated electrons from natural organic solutes in aquatic environments. *Environmental science & technology*, **1987,** *21*, (5), 485-490.
33. O'Neill, P.; Steenken, S.; Schulte-Frohlinde, D., Formation of radical cations of methoxylated benzenes by reaction with OH radicals, Ti 2+, Ag 2+, and SO 4.-in aqueous solution. An optical and conductometric pulse radiolysis and in situ radiolysis electron spin resonance study. *Journal of Physical Chemistry*, **1975,** *79*, (25), 2773-2779.

34. Neta, P.; Schuler, R. H., Rate constants for reaction of hydrogen atoms with aromatic and heterocyclic compounds. Electrophilic nature of hydrogen atoms. *Journal of the American Chemical Society*, **1972,** *94*, (4), 1056-1059.